THESIS FOR THE DEGREE OF DOCTOR OF PHILOSOPHY

Geometrical and percolative properties of spatially correlated models

Karl Olof Hallqvist Elias

UNIVERSITY OF GOTHENBURG

Division of Analysis and Probability
Department of Mathematical Sciences
University of Gothenburg
Göteborg, Sweden 2020

Geometrical and percolative properties of spatially correlated models
Karl Olof Hallqvist Elias
Göteborg 2020
ISBN: 978-91-7833-872-6 (TRYCKT)
ISBN: 978-91-7833-873-3 (PDF)
Available at: http://hdl.handle.net/2077/63419

Division of Analysis and Probability
Department of Mathematical Sciences
Chalmers University of Technology and the University of Gothenburg
SE-412 96 Göteborg
Sweden
Telephone +46 (0)31 772 1000

Typeset with LaTeX
Printed by Stema
Göteborg, Sweden 2020

Geometrical and percolative properties of spatially correlated models

Karl Olof Hallqvist Elias

Division of Analysis and Probability
Department of Mathematical Sciences
Chalmers University of Technology and the University of Gothenburg

Abstract

This thesis consists of four papers dealing with phase transitions in various models of continuum percolation. These models exhibit complicated dependencies and are generated by different Poisson processes. For each such process there is a parameter, known as the intensity, governing its behavior. By varying the value of this parameter, the geometrical and topological properties of these models may undergo dramatic and rapid changes. This phenomenon is called a phase transition and the value at which the change occur is called a critical value.

In Paper I, we study the topic of visibility in the vacant set of the Brownian interlacements in Euclidean space and the Brownian excursions process in the unit disc. For the vacant set of the Brownian interlacements we obtain upper and lower bounds of the probability of having visibility in *some* direction to a distance r in terms of the probability of having visibility in a *fixed* direction of distance r. For the vacant set of the Brownian excursions we prove a phase transition in terms of visibility to infinity (with respect to the hyperbolic metric). We also determine the critical value and show that at the critical value there is no visibility to infinity.

In Paper II we compute the critical value for percolation in the vacant set of the Brownian excursions process. We also show that the Brownian excursions process is a hyperbolic analogue of the Brownian interlacements.

In Paper III, we study the vacant set of a semi scale invariant version of the Poisson cylinder model. In this model it turns out that the vacant set is a fractal. We determine the critical value for the so-called existence phase transition and what happens at the critical value. We also compute the Hausdorff dimension of the fractal whenever it exists. Furthermore, we prove that the fractal exhibits a nontrivial connectivity phase transition for $d \geq 4$ and that the fractal is totally disconnected for $d = 2$. In the case $d = 3$ we prove a partial result showing that the fractal restricted to a plane is totally disconnected with probability one.

In Paper IV we study a continuum percolation process, the random ellipsoid model, generated by taking the intersection of a Poisson cylinder model in $\mathbb{R}^d$ and a subspace of dimension k. For $k \in \{2, 3, ..., d-2\}$, we show that there is a non-trivial phase transition concerning the expected number of ellipsoids in the cluster of the origin. When $k = d-1$ this critical value is zero. We compare these results with results obtained for the classical Poisson Boolean model.

Keywords: continuum percolation, Brownian interlacements, Brownian excursions, Poisson cylinder model, fractal percolation.

Sammanfattning

Denna avhandling består av fyra artiklar som behandlar fasövergångar i olika kontinuumperkolationsmodeller. Dessa modeller har komplicerade spatiala beroenden och genereras av olika sorters poissonprocesser. Till varje sådan process finns det en parameter som styr dess beteende. Genom att variera värdet på denna parameter kan dessa modellers geometriska och topologiska egenskaper genomgå dramatiska och snabba förändringar. Detta fenomen kallas för en fasövergång och värdet där denna fasövergång sker kallas för det kritiska värdet.

I första artikeln studeras visibilitet i den vakanta delen av molnet av brownska sammanflätningar samt molnet av brownska exkursioner. Dessa modeller beskrivs med slumpmässiga uppräkneliga mängder (moln) av brownska rörelser, varav den första definieras i euklidisk geometri medan den andra definieras i hyperbolisk geometri. I den första modellen uppskattas sannolikheten att man har visibilitet till ett avstånd r i en *godtycklig* riktning i termer av sannolikheten att man har visibilitet till ett avstånd r i en *fix* riktning. För den andra modellen uppstår istället en fasövergång för obegränsad visibilitet. Det kritiska värdet för denna fasövergång bestäms och det visas att på det kritiska värdet är sannolikheten för obegränsad visibilitet noll.

I den andra artikeln beräknas det kritiska värdet för perkolation i den vakanta delen av molnet av brownska exkursioner. I samma artikel visas även att molnet av brownska exkursioner är en hyperbol analog till molnet av brownska sammanflätningar.

Den tredje artikeln behandlar en fraktal version av Poisson cylindermodellen. Det kritiska värdet för när fraktalen går från att vara icke-tom till tom beräknas. Dessutom visas det att fraktalen är tom på det kritiska värdet. När fraktalen är icke-tom bestäms även Hausdorffdimensionen. Vidare så studeras det kritiska värdet för när fraktalen är sammanhängande. I fyra dimensioner och högre etableras en icke-trivial fasöverång. I två dimensioner visar det sig att fraktalen alltid är fullständigt osammanhängande. I tre dimensioner är fraktalen fullständigt osammanhängande då den begränsas till ett plan.

I den fjärde och sista artikeln studeras en kontinuumperkolationsmodell som fås genom att ta skärningen av en Poisson cylindermodell i $\mathbb{R}^d$ med ett underrum av dimension $k \in \{2, 3, ..., d-1\}$. Detta ger upphov till ett moln av ellipsoider i k dimensioner. För $k \in \{2, 3, ..., d-2\}$ uppvisar denna modell en icke-trivial fasövergång för det förväntade antalet ellipsoider som ligger i den sammanhängande komponenten som innehåller origo. Om $k = d-1$ så är detta kritiska värde noll. Dessa resultat jämförs därefter med liknande resultat för klassiska

kontinuumperkolationsmodeller.

List of publications

This thesis is based on the following papers:

I. **Elias, O.**, Tykesson, J. Visibility in the vacant set of the Brownian interlacements and the Brownian excursion process . *ALEA. Latin American Journal of Probability and Mathematical Statistics, 16 (2019), no. 2, 1007–1028*, doi: 10.30757/ALEA.v16-36.

II. **Elias, O.**, Tykesson, J., Viklund, F. (2019). Percolation of the vacant set of the Brownian excursions process. *Preprint*.

III. Broman, E., **Elias, O.**, Mussini, F., Tykesson, J. (2019). The fractal cylinder process: existence and connectivity phase transition. *Submitted*.

IV. **Elias, O.** (2019). Properties of a random ellipsoid model. *Submitted*.

Author contributions

I. I contributed significantly with ideas and did most of the writing.

II. I contributed significantly with ideas and did some of the writing.

III. I contributed significantly with ideas and the writing.

Acknowledgements

Foremost, I would like to express my sincerest gratitude to my advisor Johan Tykesson. Thank you for your continuous support and encouragement. Your careful and thoughtful guidance throughout these five years have been invaluable to me and has made me think twice about what really is important in mathematical research.

Besides my advisor, I would also like to thank my co-supervisors Johan Jonasson and Erik Broman as well as my co-authors Fredrik Johansson Viklund and Filipe Mussini for all the insightful discussions.

Thanks to Malin, Fanny, Jonatan, Viktor, Anna, Mikael, Erik, and everyone else that are or have been a part of Lämmeltåget. Thank you Sandra, Linnea, Edvin, Henrik, Helga, Oskar, Juan, Felix and all the other fantastic people at the institution. A special thanks to the administrative staff for all the help.

Finally, I want to thank my family and friends for all the things that makes life so great.

Thank you Filippa for making every day so much brighter.

Contents

1 Introduction

The theme of this thesis can roughly be summarized as geometrical and percolative properties of spatially correlated percolation models. These models describe random sets with complicated dependence structures. Conceptually, these are quite far from the classical percolation models such as the Bernoulli percolation model, see [BH57] and [Gri99], in which one often is able to exploit the fact that there are essentially no dependencies in the model. Models with weak dependencies can often be analyzed with similar techniques as in the models with no dependencies, but as soon as the dependencies get stronger the same type of arguments are not as easy to adapt. Thus, new type of arguments and techniques are needed to analyze these models.

The topics studied in this thesis are mainly percolation, visibility and random fractals. These subjects are studied in the context of several models of continuum percolation: Brownian interlacements, Brownian excursions, Poisson cylinders and the random ellipsoid model. In the following chapters we introduce these topics and models.

The structure of the introductory chapters is as follows. In Chapter 2 we introduce the basic theory needed to understand the appended papers. This amounts to short discussions on fractal geometry, some theory concerning hyperbolic geometry, various stochastic processes such as Poisson point processes and Brownian motion, and conformally invariant processes and the theory of conformal restriction measures. Moving on to Chapter 3 we discuss various well known models of percolation. We begin with the two simplest models, namely the Bernoulli percolation model and the Poisson Boolean model. We then move on to discussing the Mandelbrot fractal percolation model and the fractal ball model. Chapter 4 describes the models considered in the appended papers on a rather informal level. The results of the papers are then summarized Chapter 5.

The purpose of these chapters is not to give a complete historical or comprehensive background of the field, but to rather give some motivation and context of

the problems studied within this thesis.

2 Theory

This chapter covers the necessary theory needed to understand the appended papers. This amounts to rather brief discussions on various mathematical areas, such as Hausdorff dimensions, point processes and their connection with stochastic geometry, Brownian motion and its potential theory, as well as some basic theory of SLE processes and conformal restriction measures.

2.1 Notation

Throughout this thesis numerous probabilistic objects will be discussed. These will be defined on various spaces and to avoid introducing unnecessary notation, all of the probability measures will be denotes by $\mathbb{P}$. If they depend on some parameter, say x, we shall make this explicit by writing $\mathbb{P}_x$ when needed.

We denote by $B_d(x, r), r > 0$ the closed ball of radius r in $\mathbb{R}^d$ centered at $x \in \mathbb{R}^d$, and we write $B_d(r) = B_d(o, r)$ to be the ball centered at the origin. If $G = (V, E)$ is a graph, we denote by $B_G(v, n)$ the ball of radius $n \in \mathbb{N}$ in the graph metric, centered at $v \in V$.

We write Leb_k for the k-dimensional Lebesgue measure.

For a set $A \subset \mathbb{R}^d$ we let

$$A^t := A + B_d(o, t),$$

be the closed t-neighborhood of A.

The volume of a set $A \subset \mathbb{R}^d$ will be denoted by $\mathrm{Vol}\,(A)$.

2.2 Fractal geometry

The notion of fractals and self similarity is believed to have started sometime during the 17th century with Leibniz and his ilk. The first classical examples of fractals, such as the Cantor set and the Koch snowflake, appeared during the end of the 19th century and the beginning of the 20th century. The term *fractal* on the other hand first appeared in 1975 and was coined by Benoit Mandelbrot in his essay *Les objets fractals: forme, hasard et dimension*, see [Man75] as well as [Man82] for the revised and enlarged English version. For a more complete treatment on the subject of fractals we refer to [BP17, Fal14].

The easiest fractals to describe are typically generated via some iterative procedure. As introductory examples, let us consider the Cantor set and the Koch snowflake.

The Cantor set is perhaps the easiest fractal to describe. Starting with the unit interval $[0,1]$, one deletes the open middle third $\left(\frac{1}{3},\frac{2}{3}\right)$ leaving the union of two disjoint line segments: $\left[0,\frac{1}{3}\right] \cup \left[\frac{2}{3},1\right]$. Continue by deleting the open middle third of each line segment one obtains the union of four disjoint line segments: $\left[0,\frac{1}{9}\right] \cup \left[\frac{2}{9},\frac{1}{3}\right] \cup \left[\frac{2}{3},\frac{7}{9}\right] \cup \left[\frac{8}{9},1\right]$. Proceeding in this manner one obtains, in the limit, the classical Cantor set, $\mathcal{C}$.

Worth noting is that $\mathcal{C}$ is self-similar (since $\mathcal{C} = \frac{1}{3}\mathcal{C} \cup \left(\frac{1}{3}\mathcal{C} + \frac{2}{3}\right)$). Also the length of $\mathcal{C}$ is zero, but as we shall see there is a more sophisticated way of measuring its size.

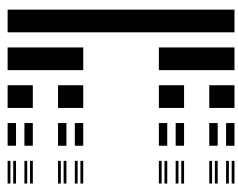

Figure 2.1: The first 5 iterations of the Cantor set

We point out, for future reference, that $\mathcal{C}$ is *totally disconnected*, meaning that all connected components are singletons.

Let us now describe the second example, the Koch snowflake. The procedure is similar to the Cantor set but instead of removing parts from a preexisting shape we now add parts to it. The construction is as follows. Start with an equilateral triangle. Replace the middle third of each side by a smaller equilateral triangle, see Figure 2.2. Repeating this procedure for each new side indefinitely one

obtains the Koch snowflake.

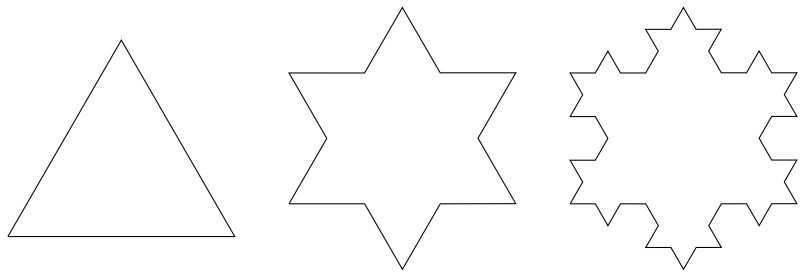

Figure 2.2: The three first iterations of the Koch snowflake

Interestingly enough, the perimeter of the Koch snowflake is infinite but the area is finite.

These two examples indicate that we ought to be a bit more careful when studying these types of objects. In particular it is of interest to study the *dimension* of these types of sets. In this thesis we consider the so-called Hausdorff dimension which we now define. For a subset $F \subset \mathbb{R}^d$, we define the s-dimensional Hausdorff measure of F to be

$$\mathcal{H}^s(F) := \lim_{\delta \to 0} \inf \left\{ \sum_{i=1}^{\infty} \operatorname{diam}(U_i)^s : \{U_i\}_{i \geq 1} \text{ is a } \delta\text{-cover of } F \right\},$$

where $\{U_i\}_{i \geq 1}$ is a δ-cover of F if $\operatorname{diam}(U_i) \leq \delta$ for every $i \geq 1$ and $F \subset \bigcup_{i=1}^{\infty} U_i$.

Next, the Hausdorff dimension of the set F is defined to be

$$\dim_{\mathcal{H}}(F) := \inf\{s > 0 : \mathcal{H}^s(F) = 0\} = \sup\{s > 0 : \mathcal{H}^s(F) = \infty\}.$$

The Hausdorff dimension is a natural extension to the classical notion of dimension in the sense that points have Hausdorff dimension 0, lines have Hausdorff dimension 1, and in general any k-dimensional subspace $S \subset \mathbb{R}^d$ has Hausdorff dimension k.

Referring back to the examples, the Cantor set has Hausdorff dimension $\log(2)/\log(3)$ while the boundary of the Koch snowflake has dimension $\log(4)/\log(3)$. Observe that the Cantor set has Hausdorff dimension strictly greater than 0 even though it is totally disconnected.

With these definitions and examples in mind one might ask what the precise definition of a fractal is. It turns out that there is no satisfactory definition

of a fractal. In fact Mandelbrots original definition (a set is a fractal if its Hausdorff dimension is strictly greater than its topological dimension) turns out to exclude "a number of sets that clearly ought to be regarded as fractals", [Fal14]. Falconer provides a less precise but a more philosophical definition of a fractal.

A set F is a fractal if it has the following properties

1. F has a fine structure, i.e. detail on arbitrarily small scales.
2. F is too irregular to be described in traditional geometrical language, locally and globally.
3. F often exhibits some type of self-similarity.
4. Usually, the "fractal dimension" of F (defined in some way) is greater than its topological dimension

2.3 The hyperbolic plane

The hyperbolic plane is essentially *the* two-dimensional manifold of negative constant curvature. In the context of percolation theory, the hyperbolic plane is often used as a stepping stone for considering classical models in a non-euclidean setting.

There are various "models" of hyperbolic geometry, but all of them are in fact isometrical to each other. The two most well known models are the Poincaré half plane model, and the Poincaré disc model. For different models and additional facts regarding hyperbolic geometry we refer to [CFKP97].

The disc model is defined by equipping the unit disc $\mathbb{D} = \{z = x + \mathrm{i}y : |z| < 1\}$ with the hyperbolic metric

$$\mathrm{d}s^2 := \frac{4}{(1-|z|^2)^2}(\mathrm{d}x^2 + \mathrm{d}y^2),$$

and the corresponding volume measure is given by

$$\mathrm{d}\mu = \frac{4}{(1-|z|^2)^2}\mathrm{d}x\mathrm{d}y.$$

We refer to $\mathbb{D}$ equipped with the metric $\mathrm{d}s^2$ as the hyperbolic plane. The

isometry group of $(\mathbb{D}, \mathrm{d}s^2)$ is given by the family of functions

$$T_{a,\lambda}(z) = \lambda \frac{z-a}{\bar{a}z-1}, \ |\lambda| = 1, |a| < 1, \tag{2.1}$$

and coincides with the group of conformal automorphisms on $\mathbb{D}$.

The hyperbolic distance between two points $\rho(u,v), u, v \in \mathbb{D}$ is given by

$$\rho(u,v) := \inf \left\{ 2 \int_0^1 \frac{|\gamma'(t)|}{1-|\gamma(t)|^2} \mathrm{d}t : \gamma \in C^1, \gamma(0) = u, \gamma(1) = v \right\},$$

and is known to be equal to

$$\rho(u,v) = 2 \tanh^{-1} \left| \frac{u-v}{1-\bar{u}v} \right|.$$

The curve that minimizes the distance is called the geodesic joining u and v. Geometrically, the geodesics corresponds to circle-segments which intersect the boundary of $\partial\mathbb{D}$ at right angles.

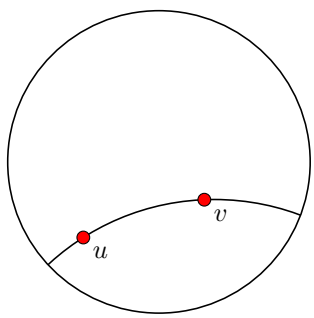

Figure 2.3: The hyperbolic geodesic between the points u and v in the Poincaré disc model.

Remark 2.3.1. *As a remark we describe a different model of the hyperbolic plane, the Poincaré half plane model. This model is defined by equipping the upper half plane* $\mathbb{H} = \{z \in \mathbb{C} : \operatorname{Im} z > 0\}$ *with the metric*

$$\mathrm{d}s^2 := \frac{\mathrm{d}x^2 + \mathrm{d}y^2}{y^2}.$$

These are seen to be isometric by applying either of the Möbius transformations

$$\begin{array}{l} \phi : \mathbb{H} \to \mathbb{D},\ z \mapsto \frac{\mathrm{i}-z}{\mathrm{i}z-1}, \\ \psi : \mathbb{D} \to \mathbb{H},\ z \mapsto \frac{\mathrm{i}+z}{1+\mathrm{i}z}. \end{array} \tag{2.2}$$

2.4 Poisson point processes and stochastic geometry

Poisson processes of various types are commonly used in percolation models and we shall see several examples of these appearing throughout the thesis. Poisson processes have numerous nice properties which make them tractable to analysis.

For further background on Poisson processes we refer to [SW08].

Definition 2.4.1. *Let X be a locally compact space and let $\mathcal{B}(X)$ denote the Borel σ-algebra on X.*

Consider the space of locally finite counting measures

$$\Omega := \left\{ \omega = \sum_{i \geq 1} \delta_{x_i} : \omega(A) < \infty, \forall A \in \mathcal{B}(X) : A \text{ compact} \right\}.$$

Let $\mathbb{P}$ be a probability measure on Ω such that

$$\mathbb{P}\left[\{\omega \in \Omega : \omega(A_i) = k_i, i = 1, ..., n\}\right] = \prod_{i=1}^{n} \frac{\mu[A_i]^{k_i}}{k_i!} \mathrm{e}^{-\mu[A_i]},$$

where $\{A_i\}_{i=1}^n \in \mathcal{M}$ is any collection of measurable disjoint sets and $k_i \in \mathbb{N}, \forall i \in \{1, 2, ..., n\}$. The random element $\omega \in \Omega$ with law $\mathbb{P}$ is said to be a Poisson process on X with intensity measure μ.

Remark 2.4.1. *Alternatively, we say that a random element $\omega \in \Omega$ is a Poisson point process on X if for any sequence of disjoint sets $A_i, 1 \leq i \leq n$ the random variables $(\omega(A_i))_{1 \leq i \leq n}$ are independent and Poisson distributed with parameter $\mu(A_i)$.*

Let us now discuss some examples of some classical Poisson point processes.

Example 2.4.1. *The standard Poisson point process on $\mathbb{R}^d$ is obtained by letting $X = \mathbb{R}^d$ and taking the intensity measure to be the Lebesgue measure, $\mu = \lambda \cdot \mathrm{Leb}_d, \lambda > 0$.*

Remark 2.4.2. *The Poisson point process in $\mathbb{R}^d$ can locally be described as follows. Let $A \Subset \mathbb{R}^d$ be a compact subset with non-empty interior. Let $N_A = \omega(A)$ be the number of points contained in A. Conditioned on N_A, the points $x_1, ..., x_n \in \text{supp}\ (\omega)$ are then i.i.d with distribution*

$$\mathbb{P}(x_i \in B) = \frac{\text{Leb}_d(B \cap A)}{\text{Leb}_d(A)}.$$

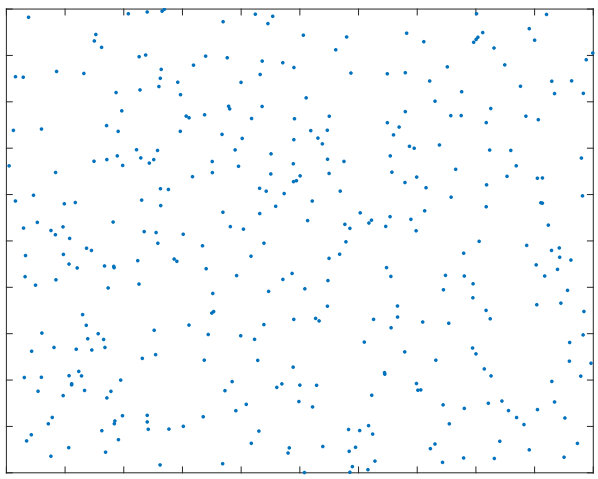

Figure 2.4: A simulation of the Poisson point process in $\mathbb{R}^2$.

A different example that will be of use when defining the Poisson cylinder process is the Poisson line process.

Example 2.4.2. *Let $A(2,1)$ be the space of affine lines on $\mathbb{R}^2$ and let ν_2 be the unique (up to scaling) measure on $A(2,1)$ which is invariant under translations and rotations. The Poisson line process is a Poisson point process on the space $A(2,1)$ with intensity measure ν_2.*

If we parametrize a line $L \in A(2,1)$ in two dimensions by

$$L(a,p) = \{(a,1)t + (p,0)\}_{t\in\mathbb{R}}, a, p \in \mathbb{R}.$$

Then ν_2 is given by

$$\mathrm{d}\nu_2(p,a) = \frac{1}{(1+a^2)^{3/2}}\mathrm{d}a\mathrm{d}p.$$

Figure 2.5: A simulation of the Poisson line process in $\mathbb{R}^2$. Different colors represent different lines.

It might clear from Figures 2.4 and 2.5 that the Poisson processes in these examples can be viewed as random sets in some sense. The precise definition is as follows.

Definition 2.4.2. *Let Σ be the family of closed sets in $\mathbb{R}^d$. Let $\mathbb{F}$ be the σ-algebra generated by the families*

$$\mathcal{F}_K := \{F \in \Sigma : F \cap K \neq \emptyset\}, \ K \text{ compact.}$$

A random closed set is a Σ-valued random variable.

Remark 2.4.3. *We now describe how the Poisson line process on $A(2,1)$ induces a random closed set (see Example 2.4.2). The union of the lines contained in the support* $\operatorname{supp}(\omega)$ *defines a random closed set in $\mathbb{R}^2$ by*

$$\mathcal{S}(\omega) := \bigcup_{L \in \operatorname{supp}(\omega)} L, \tag{2.3}$$

see Figure 2.5. Moreover, the law of $\mathcal{S}$ is determined by

$$\mathbb{P}[\mathcal{S} \cap K = \emptyset] = \mathbb{P}[\omega(\mathcal{L}_K) = 0] = \mathrm{e}^{-\nu_2(\mathcal{L}_K)}, \tag{2.4}$$

where

$$\mathcal{L}_K = \{L \in A(2,1) : L \cap K \neq \emptyset\}$$

is the set of all lines that intersect K. A similar but easier construction holds for the Poisson point process in Example 2.4.2.

In Chapters 3 and 4 we will see more examples of how Poisson processes generate random sets.

2.5 Brownian motion

Brownian motion or the Wiener process is the canonical mathematical model describing diffusion. There are numerous ways of characterizing Brownian motion, for instance as a scaling limit of the simple random walk, or as the Markov process with semi-group defined by the solution to the heat equation or even as the Gaussian process $(W_t)_{t\geq 0}$ with covariance $\mathbf{Cov}(W_t, W_s) = t \wedge s$. For a more in depth discussion concerning these topics we refer to [MP10, Szn98].

The standard definition of the one-dimensional Brownian motion is as follows. First recall that a random variable X is normally distributed with mean μ and variance σ^2 if its distribution function is given by

$$\mathbb{P}_{\mu,\sigma}\left[X \leq x\right] = \frac{1}{\sqrt{2\pi\sigma^2}} \int_{-\infty}^{x} \exp\left\{-\frac{(t-\mu)^2}{2\sigma^2}\right\} \mathrm{d}t, \forall x \in \mathbb{R}. \tag{2.5}$$

The definition of Brownian motion is given below.

Definition 2.5.1. *A stochastic process $\{W(t) : t \geq 0\}$ is a one-dimensional Brownian motion started at $x \in \mathbb{R}$ if $W(0) = x$ and*

- *For all times $0 \leq t_1 \leq t_2 .... \leq t_n$ the increments $W(t_{j+1}) - W(t_j), j = 1, 2, ..., n-1$ are independent random variables, and are normally distributed with mean 0 and variance $t_j - t_{j-1}$.*
- *The function $t \mapsto W(t)$ is almost surely continuous.*

If $W_1, W_2, ..., W_d$ are independent Brownian motions started at

$$W_1(0) = x_1, W_2(0) = x_2, ..., W_d(0) = x_d,$$

respectively, we then say that the vector

$$W(t) := (W_1(t), ..., W_d(t))$$

is a d-dimensional Brownian motion started at $x = (x_1, ..., x_d) \in \mathbb{R}^d$.

The fact that Brownian motion exists is a highly non-trivial fact and the first proof of this fact is attributed to Norbert Wiener, see [Wie23], and a contemporary proof can be found in [MP10].

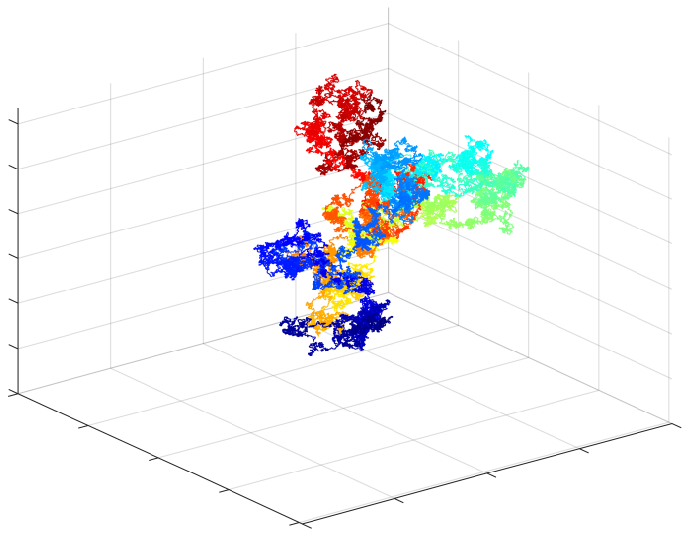

Figure 2.6: A simulation of the Brownian motion in $\mathbb{R}^3$. The color gradient (starting from blue and ending at red) describes the evolution of the Brownian motion.

Remark 2.5.1. *In the context of the Brownian interlacements and the Brownian excursions process (which we will encounter in later chapters) we will mainly be considering the graphs of Brownian motions rather than the random curves evolving in time.*

We shall now introduce some notions from potential theory. In order to do so we shall need some preliminary definitions. The transition density, $p(t, x, y)$, of Brownian motion is defined by the equation

$$\mathbb{P}_x [W(t) \in A] := \mathbb{P} [W(t) \in A | W(0) = x] = \int_A p(t, x, y) \mathrm{d}y, A \subset \mathbb{R}^d \tag{2.6}$$

and since $W(t)$ is a normally distributed variable it follows that $p(t, x, y)$ is given by

$$p(t, x, y) = \frac{1}{(2\pi t)^{d/2}} \exp\left\{-\frac{1}{2t} |x - y|^2\right\}. \tag{2.7}$$

The Greens function, whenever it exists, is defined by

$$G(x,y) := \int_0^\infty p(t,x,y)\mathrm{d}t = \begin{cases} \frac{\Gamma(d/2-1)}{2\pi^{d/2}} |x-y|^{-d+2}, & d \geq 3, \\ \infty & d = 1,2. \end{cases} \tag{2.8}$$

The hitting time of a set $K \subset \mathbb{R}^d$ is the first time that the Brownian motion hits K

$$H_K := \inf \{t > 0 : W(t) \in K\}, \tag{2.9}$$

and the last exit time of a set K is defined by

$$L_K := \sup \{t > 0 : W(t) \in K\}. \tag{2.10}$$

Note that $H_K < \infty$ if and only if $L_K > 0$.

Remark 2.5.2. *The fact that $G(x,y) = \infty,\ \forall x, y$ if $d \leq 2$ is due to the fact that Brownian motion is recurrent for $d \leq 2$.*

We are now ready to discuss the potential theoretic framework needed. For a set K we let

$$E_K(\lambda) = \int_{K\times K} G(x,y)\lambda(\mathrm{d}x)\lambda(\mathrm{d}y)$$

denote the Newtonian energy of a probability measure λ supported on the set K. The capacity is defined by the inverse of the minimal Newtonian energy

$$\mathrm{cap}(K) = \left\{ \inf_{\lambda:\lambda(K)=1} E_K(\lambda) \right\}^{-1}. \tag{2.11}$$

The minimizer, when it exists, is denoted by e_K and is called the equilibrium measure of K. It can be shown that e_K is supported on the boundary ∂K and that $e_K(K) = \mathrm{cap}(K)$.

Example 2.5.1. *If $K = B_d(x,r)$ then the normalized equilibrium measure, $\tilde{e}_K = \frac{1}{\mathrm{cap}(K)} e_K$, is given by*

$$\tilde{e}_K = \sigma_r,$$

where σ_r is the uniform probability measure on $\partial B_d(x,r)$. Moreover,

$$\mathrm{cap}(B_d(x,r)) = \frac{2\pi^{d/2}}{\Gamma(d/2-1)} r^{d-2}. \tag{2.12}$$

It is a classical fact, due to Kakutani [Kak44], that $\mathrm{cap}(K) > 0$ if and only if $\mathbb{P}_x[H_K < \infty] > 0,\ \forall x \in \mathbb{R}^d$. Moreover, the equilibrium measure is related to

the hitting time and last exit time by

$$e_{K_1}(\mathrm{d}y) = \int \mathbb{P}_x \left[W(H_K) \in \mathrm{d}y, H_K < \infty \right] e_{K_2}(\mathrm{d}x), \ K_1 \subset K_2, \tag{2.13}$$

$$\mathbb{P}_x \left[W(L_K) \in \mathrm{d}y, L_K > 0 \right] = G(x,y) e_K(\mathrm{d}y). \tag{2.14}$$

In particular, Equation (2.13) implies that if $W(0)$ is a started according to $\tilde{e}_{K_2} := \frac{1}{\mathrm{cap}(K_2)} e_{K_2}$ then the probability of hitting K_1 is simply given by

$$\int \mathbb{P}_x \left[H_{K_1} < \infty \right] \tilde{e}_{K_2}(\mathrm{d}x) = \frac{\mathrm{cap}(K_1)}{\mathrm{cap}(K_2)} \tag{2.15}$$

2.6 A brief discussion on the theory of conformal restrictions and SLE

This section contains a brief discussion on the theory of conformal restriction and SLE processes. For a more in depth discussion concerning these topics we refer to [Wu15], [Wer05], [LSW03] and Chapter 9 in [Law05].

Schramm-Loewner evolution, introduced by Oded Schramm in [Sch00], describes a conformally invariant random growth process of a set $K_t, t \geq 0$ in a simply connected domain $D \subset \mathbb{C}$. To be precise, suppose that $D = \mathbb{H}$ is the half plane and let $\xi(t) := W(\kappa t), \kappa \geq 0$, where W is a one-dimensional Brownian motion with $W(0) = 0$. The SLE(κ) process is then defined as follows.

For $z \in \mathbb{H} \setminus \{0\}$, let $g_t(z)$ be the solution to the ODE

$$\partial_t g_t(z) = \frac{2}{g_t(z) - \xi(t)}, g_0(z) = z, \tag{2.16}$$

and note that this is well defined up to the time

$$T(z) := \sup \left\{ t \geq 0 : \min_{s \in [0,t]} |g_s(z) - \xi(t)| > 0 \right\}.$$

Let $K_t := \{z \in \mathbb{H} : T(z) \leq t\}$ and let $\mathbb{H}_t$ be the unbounded component of $\mathbb{H} \setminus K_t$. It is known that K_t is bounded and that g_t is a conformal map from $\mathbb{H}_t$ onto $\mathbb{H}$. The collection of conformal maps $(g_t)_{t \geq 0}$ is then called the chordal SLE(κ).

The SLE(κ) curve is then defined by

$$\gamma(t) := \lim_{y \downarrow 0} g_t^{-1}(\xi(t) + \mathrm{i}y).$$

It should be noted that for $\kappa \in (0, 4]$ the random curve $\gamma(t)$ in fact is a simple curve, see [RS05]. Moreover, the almost sure Hausdorff dimension of $\gamma(t)$ is $\min\left(1 + \frac{\kappa}{8}, 2\right)$, [Bef08].

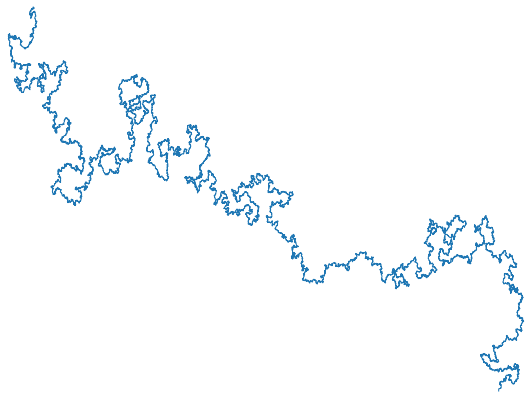

Figure 2.7: A simulation of the SLE(8/3) curve. The curve was generated using the code by [Fos19] which is based on the algorithm developed in [FLM19] .

For an arbitrary simply connected domain D with points $x, y \in \partial D$, the chordal SLE(κ) from x to y in D can be defined in the following manner. Let $\phi : \mathbb{H} \to D$ be any conformal map such that $\phi(0) = x, \phi(\infty) = y$, then the chordal SLE($\kappa$) in D is defined as the image of the chordal SLE(κ) in $\mathbb{H}$ from 0 to ∞ under ϕ.

It is worth commenting that the SLE(κ) curves are in fact the only random curves satisfying the following properties:

1. **Conformal Invariance:** If γ is an SLE curve in D from x to y and $\phi : D \mapsto D'$ is a conformal map, then $\phi(\gamma)$ has the same distribution as an SLE curve in D' from $\phi(x)$ to $\phi(y)$.

2. **Domain Markov Property:** If γ is an SLE curve in a domain D. Then given $\gamma([0, t])$ the remaining curve $\gamma([t, \infty])$ is an SLE(κ) curve in $D \setminus \gamma([0, t])$.

We shall need a variant of the standard SLE(κ) process called the SLE(κ, ρ) introduced in Section 8 of [LSW03]. Suppose $\rho > -2$ and let W_t be a standard one-dimensional Brownian motion. Let Z_t denote the solution of the stochastic

differential equation

$$\mathrm{d}Z_t = \frac{\rho+2}{Z_t}\mathrm{d}t + \sqrt{\kappa}\mathrm{d}W_t,\ Z_0 = z \geq 0,$$

and let

$$O_t = -\int_0^t \frac{2}{Z_u}\mathrm{d}u,\ O_0 = 0,$$

We remark that $Z_t \overset{d}{=} \sqrt{\kappa}Y_t$ where Y_t is a so-called d-dimensional Bessel process with

$$d = 1 + \frac{2(\rho+2)}{\kappa}.$$

By letting $\xi(t) = Z_t + O_t$ the resulting solution to Equation (2.16) is the SLE(κ, ρ) process in $\mathbb{H}$ started from $(0, z)$. The point z is referred to as a force point and ρ is thought of as a charge or weight that is associated with z. Conceptually, ρ describes the attraction ($\rho < 0$) and repulsion ($\rho > 0$) to and from the boundary.

We now move on to discussing the theory of restriction measures. As is standard, we shall give the definition on the upper half plane $\mathbb{H}$. Before we can give the full definition we shall need some additional concepts.

Let $\mathcal{A}_c$ be the collection of all bounded closed subsets $A \subset \overline{\mathbb{H}}$ such that

$$0 \notin A, A = \overline{A \cap \mathbb{H}}, \quad \text{and } \mathbb{H} \setminus A \text{ is simply connected.}$$

and let Ω^+ denote the family of closed sets $K \subset \overline{\mathbb{H}}$ such that

$$K \cap \mathbb{R} = (-\infty, 0],\ K \text{ and } \mathbb{H} \setminus K \text{ is connected .}$$

Moreover, let $\mathcal{A}_c^+ = \{A \in \mathcal{A}_c : A \cap \mathbb{R} \subset (0, \infty)\}$. We equip Ω^+ with the σ-field generated by the sets $[K \in \Omega^+ : K \cap A = \emptyset]$ where $A \in \mathcal{A}_c^+$, c.f Definition 2.4.2.

Let $\Phi_A : \mathbb{H} \setminus A \mapsto \mathbb{H}$ be the conformal map such that

$$\Phi_A(0) = 0,\ \Phi_A(\infty) = \infty, \lim_{z\to\infty} \Phi_A(z)/z = 1$$

.

Definition 2.6.1. *A random element K on Ω^+ has the right-sided restriction property if*

1. *$\lambda K \overset{d}{=} K$ for any $\lambda > 0$*
2. *For any $A \in \mathcal{A}_c^+$, the conditional law of $\Phi_A(K)$ on the event $K \cap A = \emptyset$*

coincides with K.

Any probability measure satisfying the conditions is called a one-sided restriction measure.

Remark 2.6.1. *The second item of this definition should be understood in terms of the pushforward of the measure corresponding to the law of the random set K. That is*

$$\mathbb{P}\left[\Phi_A^{-1}(K) \in \cdot\right] = \mathbb{P}\left[K \in \cdot | K \cap A \neq \emptyset\right]$$

It turns out that these two conditions are very restrictive. In fact for any one-sided restriction measure there exists a $\alpha > 0$ such that

$$\mathbb{P}\left[K \cap A \neq \emptyset\right] = \Phi_A(0)^\alpha. \tag{2.17}$$

Hence the family of one-sided restriction measures corresponds to a one-parameter family of measures $\mathbb{P}_\alpha$. We point out that since the events $K \cap A \neq \emptyset$ generate the σ-algebra, Equation (2.17) determines any such $\mathbb{P}_\alpha$ uniquely.

We comment that there is a two-sided analogy to the one-sided restriction measures (which are often just referred to as conformal restriction measures). In particular the law of an SLE(8/3) coincides with the restriction measure with exponent $\alpha = 5/8$, see Theorem 6.1 in [LSW03].

Example 2.6.1. *An example that is of great importance to Paper II is that the right-side boundary of a one-sided restriction measure with exponent β coincides with the law of a* SLE$(8/3, \rho)$ *where ρ and β is related via the equation*

$$\rho(\beta) = \frac{1}{3}\left(-8 + 2\sqrt{24\beta + 1}\right). \tag{2.18}$$

3 Percolation

Let us begin with two seemingly distinct questions

- Suppose that a porous stone is submerged in water. How likely is it that the water reaches the center of the stone?
- Given some type of wireless communication system, how can we quantify the coverage and connectivity of this system?

The unifying theme of these questions is that they both can be analyzed with methods in percolation theory.

The first question is perhaps *the* one that initialized the entire mathematical field of percolation. The first concrete model is is due to Hammersley and Broadbent [BH57] and is commonly referred to as the Bernoulli percolation model. The second question led E.N Gilbert to introduce the classical Poisson Boolean model, [Gil61, Gil65], as a simple model for spatial networks.

Despite being motivated by questions in physics and communications theory, the applications to other areas of science are manifold, see for instance [Bal87, Sah94] and the references therein.

3.1 Bernoulli percolation

The first and perhaps the most fundamental model of percolation is the Bernoulli percolation model. Since its inception, the Bernoulli percolation model has received a great deal of attention within the probabilistic community and has inspired the creation of similar models such as first-passage percolation and bootstrap percolation, see [HW65, CLR79]. For a more complete treatment of the Bernoulli percolation model we refer to the books [Gri99, BR06].

First we describe the model informally. Consider the hexagonal lattice in Figure 3.1. For each face of the lattice, flip a coin. If it turns up heads color the face red, and otherwise color the face white.

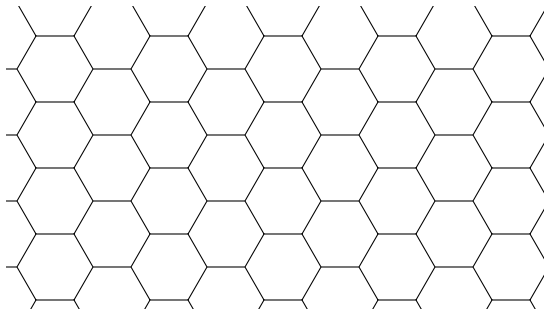

Figure 3.1: A slice of the hexagonal lattice

Proceeding in this manner typically three different pictures or *phases* emerge. These naturally depend on the probability that the coin shows heads, denoted by p, as well as on the geometry of the underlying graph. What characterizes these phases are three distinct topological behaviors. In the language of percolation theory these phases are referred to as the *subcritical phase*, *critical phase* and, the *supercritical phase*.

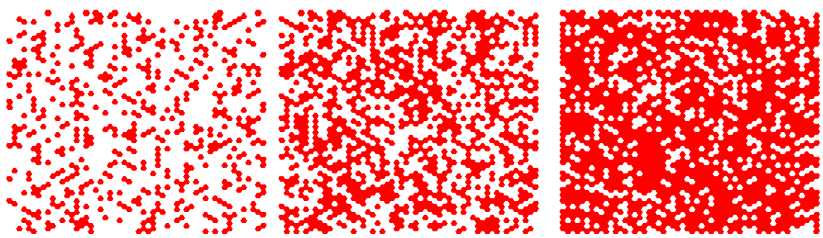

Figure 3.2: Bernoulli percolation on the faces of the hexagonal lattice. From left to right: Subcritical, critical, supercritical.

In the subcritical phase the connected components of red vertices are finite almost surely and the cluster radius distribution has an exponential tail. In the supercritical phase (in this example) there is one unique system-spanning cluster and the probability that one can find a self-avoiding path of infinite length from a given vertex consisting of red vertices is strictly positive. In the critical phase not much is known beyond the two-dimensional world and the

high-dimensional world ($d \geq 11$), see for instance [Wer09] and [HS90, HvdH17] respectively.

We now rigorously define the model. The Bernoulli site percolation model on a given graph $G = (V, E)$ is defined by the probability measure $\mathbb{P}_p$ on the space of configurations $\Omega_G = \{0, 1\}^V$ where

$$\mathbb{P}_p = \prod_{v \in V} p\delta_1 + (1 - p)\delta_0. \tag{3.1}$$

For a configuration $\omega \in \Omega_G$ we say that a site is open if $\omega(v) = 1$ and closed if $\omega(v) = 0$. For two sets $A, B \subset V$ we write $A \overset{\omega}{\leftrightarrow} B$ to mean the event that there is a nearest neighbour path in V only using open vertices in ω.

Given a graph $G = (V, E)$ and a vertex $o \in V$, we denote by

$$C_o(\omega) = \left\{ v \in V : o \overset{\omega}{\leftrightarrow} v \right\},$$

the set of all vertices $v \in V$ that can be reached from o using a nearest neighbor path consisting of open sites. For simplicity, we shall assume that the graph is transitive, which essentially means that the vertices are indistinguishable from one another. The percolation probability, $\theta(p)$, can then be defined by

$$\theta(p) = \mathbb{P}_p \left(\omega \in \Omega : |C_o(\omega)| = \infty \right). \tag{3.2}$$

Remark 3.1.1. *There is a natural coupling in the Bernoulli percolation model between different values of p. Let $U_v, v \in V$, be a family of independent uniformly distributed random variables on $[0, 1]$ and define the configuration*

$$\omega_v^p := \begin{cases} 1, & \text{if } U_v \leq p \\ 0, & \text{else}, \end{cases} \tag{3.3}$$

for all $v \in V$. Then ω^p has the same distribution as a Bernoulli percolation model with parameter p and if $p \leq q$ then $\omega_v^p \leq \omega_v^q$ for all $v \in V$. Using this coupling it is clear that $\theta(p)$ is increasing in p.

The perhaps most fundamental question in percolation theory is to establish the presence of a critical value $p_c \in [0, 1]$ such that

$$\theta(p) = 0, p < p_c, \tag{3.4}$$
$$\theta(p) > 0, p > p_c. \tag{3.5}$$

Mathematically, p_c is defined by

$$p_c := \sup \{p \in [0,1] : \theta(p) = 0\}.$$

The remainder of this section will be devoted to site percolation on the triangular lattice, which is equivalent to percolation on the faces of the hexagonal lattice. Many of the results mentioned here holds in far greater generality and we refer to [Gri99, BR06] for more of these facts. For the triangular lattice we have the following result.

Theorem 3.1.1. $p_c = 1/2$

The first theorem of this type is due to Kesten in [Kes80] and was proven for the bond percolation model on $\mathbb{Z}^2$. In general the quantity p_c is not known other than in some two-dimensional cases and typically there is nothing special to be inferred from the specific value. It is often more interesting to understand the different qualitative and quantitative behaviors of the specific phases. As an example we define $\theta_n(p) := \mathbb{P}_p\left(o \overset{\omega}{\leftrightarrow} \partial B_G(o,n)\right)$, then we have the following known result, see [Kes80, Men86].

Theorem 3.1.2. *Consider Bernoulli percolation on the triangular lattice. Then*

$$\theta_n(p) \leq \mathrm{e}^{-c(p)n}, \forall p < p_c,$$
$$\theta(p_c) = 0.$$

Moreover, for $p > p_c$ the infinite cluster is unique.

We point out that the statement $\theta(p_c) = 0$ is a consequence of planarity and it is not known, though conjectured, whether the same holds in a more general setting. In particular, it is longstanding question whether $\theta(p_c) = 0$ holds for the hypercubic lattice $\mathbb{Z}^3$. Whenever this is true however, the phase transition is said to be *continuous*. The statement that the infinite cluster is unique is a consequence of the classical Burton-Keane argument, [BK89].

In the field of percolation one is often interested in other quantities than $\theta(p)$. Two frequently appearing are

$$\chi(p) := \mathbb{E}_p\left[|\mathcal{C}_o(\omega)|\right], \tilde{\theta}_n(p) = \mathbb{P}_p\left[B_G(o,n) \overset{\omega}{\leftrightarrow} B_G(o,2n)^c\right].$$

Note that if $p > p_c$ then $\chi(p) = \infty$ since with strictly positive probability $|\mathcal{C}_o| = \infty$. Similarly, if $p > p_c$ then $\tilde{\theta}_n(p) > 0$ since we trivially have

$$\theta_{2n}(p) \leq \tilde{\theta}_n(p).$$

In analogy with p_c one can ask if there exist critical values p_N, p_{cross} defined by

$$p_N := \sup\{p \in [0,1] : \chi(p) < \infty\}, \tag{3.6}$$

$$p_{\text{cross}} := \sup\left\{p \in [0,1] : \liminf_{n\geq 1} \tilde{\theta}_n(p) = 0\right\}. \tag{3.7}$$

A rather remarkable fact about the Bernoulli percolation model is that all of the critical values above coincide, see [DCT16] for a short proof of this fact.

Theorem 3.1.3.

$$p_c = p_N = p_{\text{cross}}$$

Whenever this type of phenomenon occurs, the phase transition is said to be *sharp*.

3.2 Boolean percolation

The Poisson Boolean percolation model, sometimes referred to as the Gilbert disc model, is the simplest percolation model defined on a continuous space. Similar to the Bernoulli percolation model, this model also exhibits three phases, though they are far less understood.

The Poisson Boolean model is defined as a Poisson point process on

$$\Omega_B := \left\{\omega = \sum_{i\geq 1} \delta_{(x_i,r_i)} : \omega(K \times \mathbb{R}_+) < \infty, \forall K \subset \mathbb{R}^d \text{ compact}\right\}, \tag{3.8}$$

where the first coordinate represents the center of a ball and the second corresponds to the random radius of a ball.

The intensity measure for a given $\lambda > 0$ is given by

$$\mu = \lambda \cdot \text{Leb}_d \times \rho,$$

where ρ is a probability measure on $\mathbb{R}_+$. The random structures one wants to study is the occupied set, $\mathcal{O}$, and the vacant set, $\mathcal{V}$, defined by

$$\mathcal{O} = \mathcal{O}(\omega) := \bigcup_{(z,r)\in \text{supp}(\omega)} B_d(z,r), \mathcal{V} := \mathbb{R}^d \setminus \mathcal{O}. \tag{3.9}$$

It is well known, see Proposition 7.3 in [MR96], that

$$\mathbb{P}\left[\mathcal{O} = \mathbb{R}^d\right] = 1 \Leftrightarrow \int_0^\infty r^d \rho(\mathrm{d}r) = \infty.$$

Hence for the model to be non-trivial one must assume that

$$\int_0^\infty r^d \rho(\mathrm{d}r) < \infty. \tag{3.10}$$

Observe that this quantity corresponds to the expected volume of a ball with radius distributed according to ρ.

Furthermore, using the definition of a random closed set, we see that the law of the occupied and vacant set is determined by the quantity

$$\begin{aligned}\mathbb{P}_\lambda\left[\mathcal{O} \cap K = \emptyset\right] &= \mathbb{P}_\lambda\left[K \subset \mathcal{V}\right] = \mathbb{P}_\lambda\left[\omega((z,r) : B_d(z,r) \cap K \neq \emptyset) = 0\right] \\ &= \exp\left\{-\lambda\left(\mathrm{Leb}_d \times \mu\right)\left[(z,r) : B_d(z,r) \cap K \neq \emptyset\right]\right\} \end{aligned} \tag{3.11}$$

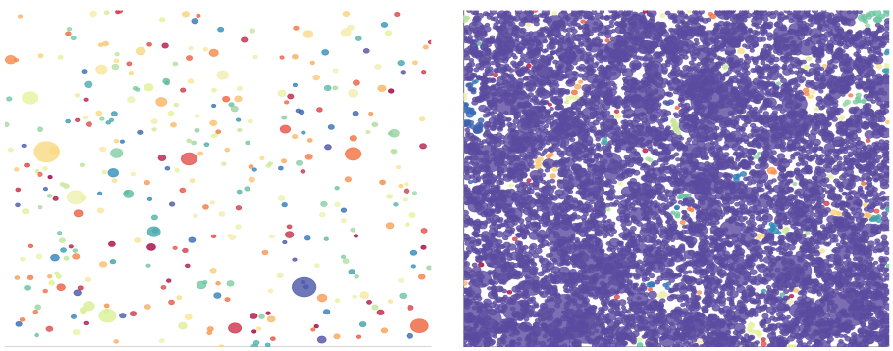

Figure 3.3: Boolean percolation in $\mathbb{R}^2$ with centers in the square $[-100, 100]^2$ and intensities $\lambda = 0.01$ and $\lambda = 0.2$ respectively. Different colors represents different clusters. The balls represent the occupied set and the white part corresponds to the vacant set.

One main conceptual difference between the Bernoulli percolation and the Boolean percolation is that the occupied and vacant sets are qualitatively different. This is not the case if one compares the open and closed sites of a Bernoulli percolation model.

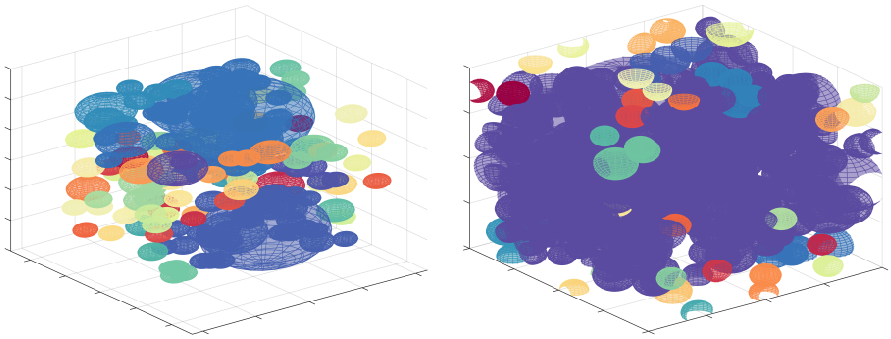

Figure 3.4: Boolean percolation in $\mathbb{R}^3$ with centers in the box $[-10, 10]^3$ and intensities $\lambda = 0.025$ and $\lambda = 0.05$ respectively. Different colors represent different clusters. The balls represent the occupied clusters and the white part corresponds to the vacant set.

For $A, B \subset \mathbb{R}^d$ define $A \overset{\mathcal{O}}{\leftrightarrow} B$ (and $A \overset{\mathcal{V}}{\leftrightarrow} B$) to be the event that there exists a path contained in $\mathcal{O}$ (respectively in $\mathcal{V}$) connecting the sets A and B. Moreover, we define

$$\left\{o \overset{\cdot}{\leftrightarrow} \infty\right\} = \cap_{n\geq 1} \left\{o \overset{\cdot}{\leftrightarrow} \partial B_d(n)\right\}.$$

In analogy with the Bernoulli model we define the two quantities

$$\theta(\lambda) := \mathbb{P}_\lambda \left[o \overset{\mathcal{O}}{\leftrightarrow} \infty\right], \tag{3.12}$$

$$\theta^\star(\lambda) := \mathbb{P}_\lambda \left[o \overset{\mathcal{V}}{\leftrightarrow} \infty\right]. \tag{3.13}$$

We comment that using a similar coupling to that of the Bernoulli percolation model one can show that $\theta(\lambda)$ is increasing while $\theta^\star(\lambda)$ is decreasing in λ. In this setting the first question to address is the presence of the critical values $\lambda_c, \lambda_c^\star \in [0, \infty]$ defined by

$$\lambda_c = \sup\{\lambda > 0 : \theta(\lambda) = 0\}, \tag{3.14}$$

$$\lambda_c^\star = \inf\{\lambda > 0 : \theta^\star(\lambda) = 0\}. \tag{3.15}$$

Remark 3.2.1. *It should be relatively clear that since radius of the spheres in the Boolean model can be arbitrarily large the spatial dependencies are much stronger than in the Bernoulli percolation model. In fact a short computation shows that the probability that the origin $o \in \mathbb{R}^d$ is connected to the boundary of*

the ball $\partial B_d(R)$ can be bounded from below by:

$$\begin{aligned}\mathbb{P}_\lambda\left[o \overset{\mathcal{O}}{\leftrightarrow} \partial B_d(R)\right] &\geq \mathbb{P}_\lambda\left[\omega\left[(z,r) : o \in B_d(z,r), r \geq 2R\right] \geq 1\right] \\ &= 1 - \exp\left\{-\lambda \int \mathrm{I}\left\{o \in B_d(z,r), r \geq 2R\right\} \mathrm{d}z\mathrm{d}\rho(r)\right\} \\ &= 1 - \exp\left\{-\lambda \int_{r \geq 2R} \mathrm{Vol}\left(B_d(r)\right)\mathrm{d}\rho(r)\right\} \\ &\geq c\lambda \int_{r \geq 2R} r^d \mathrm{d}\rho(r).\end{aligned}$$

In particular as $R \to \infty$ this quantity can under assumption (3.10) *decay arbitrarily slow.*

These types of dependencies indicates that the approach to proving the presence of a non-trivial phase transition concerning percolation can be conceptually different for the Boolean percolation model when compared to the Bernoulli percolation model.

The techniques for proving the non-triviality of λ_c and $\lambda_c^\star$ relies on introducing values similar to p_N and p_{cross}. Thus we first define

$$\mathcal{C}_o = \left\{x \in \mathbb{R}^d : o \overset{\mathcal{O}}{\leftrightarrow} x\right\}$$

the occupied cluster containing the origin. The analogue of p_N is then given by

$$\lambda_N = \sup\left\{\lambda > 0 : \mathbb{E}_\lambda\left[\#\mathcal{C}_o\right] < \infty\right\}, \tag{3.16}$$

where $\#\mathcal{C}_o$ denotes the cardinality of the set $\{(x,r) \in \omega : B_d(x,r) \subset \mathcal{C}_o(\omega)\}$. The first result concerning this threshold was due to Hall who established the equivalence

$$\lambda_N \in (0,\infty) \Leftrightarrow \int_0^\infty r^{2d} \rho(\mathrm{d}r) < \infty,$$

in [Hal85].

Analogous to p_{cross} one also needs to consider the following critical values

$$\lambda_{\mathrm{cross}} = \inf\left\{\lambda > 0 : \inf_{r>0} \mathbb{P}_\lambda\left[B_d(r) \overset{\mathcal{O}}{\leftrightarrow} B_d(2r)^c\right] > 0\right\}, \tag{3.17}$$

$$\lambda_{\mathrm{cross}}^\star = \inf\left\{\lambda > 0 : \inf_{r>0} \mathbb{P}_\lambda\left[B_d(r) \overset{\mathcal{V}}{\leftrightarrow} B_d(2r)^c\right] > 0\right\}. \tag{3.18}$$

For the reader well-versed in percolation theory, the reason why these quantities

are introduced is that they enables one to initialize renormalization schemes.

It was not until 2008 that $\lambda_c > 0$ was established by Gouéré in [Gou08] under the minimal assumption (3.10). To establish $\lambda_c^\star > 0$ it took roughly another 10 years and the result is due to Ahlberg, Tassion and Teixeira in [ATT18a].

The sharpness phenomenon in the Boolean percolation model is much less understood than in the Bernoulli case. In the bounded radii case it is known that $\lambda_c = \lambda_{\text{cross}} = \lambda_N$, see [Zie18] for a contemporary proof. In the unbounded radii case, Duminil-Copin, Raoufi and Tassion established the following result in [DRT18].

Theorem 3.2.1. *If*

$$\int_0^\infty r^{5d-3}\rho(\mathrm{d}r) < \infty$$

then $\lambda_{\text{cross}} = \lambda_c$.

For $d = 2$ Ahlberg, Tassion, and Teixeira established in [ATT18b] a result similar to what is known for the Bernoulli percolation model.

Theorem 3.2.2. *If*

$$\int_0^\infty r^2\rho(\mathrm{d}r) < \infty$$

then $\lambda_c = \lambda_c^\star$.

For $d \geq 3$ the equality does not hold, see [Sar97]. In fact for $d \geq 3$ there is a non-empty open interval of intensities in which both the vacant and the occupied set percolate. A similar result holds for Bernoulli percolation as well, see [CR85].

We now turn to a short discussion that highlights some of the differences that appear in the Boolean percolation model on $\mathbb{R}^d$ and $\mathbb{H}^2$ respectively.

The unit radius version of the Poisson Boolean model in $\mathbb{H}^2$ is defined by first considering a Poisson point process on $\mathbb{H}^2$ with intensity measure $\lambda\mu_{\mathbb{H}}$ where $\mu_{\mathbb{H}}$ is the volume measure on $\mathbb{H}^2$. At each Poisson point one places a ball of unit radius (in the hyperbolic metric). The occupied set $\mathcal{O}_{\mathbb{H}}$ is then defined analogously as the union of all such balls while the vacant is the complement of $\mathcal{O}_{\mathbb{H}}$.

For the purpose of this discussion, let us introduce the following critical values. The first is whether the occupied and vacant set contains a *unique* connected component. Let $N_{\mathcal{O}}$ and $N_{\mathcal{V}}$ denote the number of unbounded connected

components contained within $\mathcal{O}_{\mathbb{H}}$ and $\mathcal{V}_{\mathbb{H}}$ respectively. Define

$$\lambda_u := \inf\{\lambda > 0 : \mathbb{P}_\lambda[N_{\mathcal{O}} = 1] = 1\}, \tag{3.19}$$

Let $\lambda_c, \lambda_c^\star$ denote the critical values for percolation in the vacant and occupied set. Note that for $\lambda > \lambda_c$ (and $\lambda < \lambda_c^\star$) we have that $N_{\mathcal{O}} > 0$ ($N_{\mathcal{V}} > 0$) occurs with probability one.

In $\mathbb{R}^d$ it is a well known fact that λ_u coincides with the standard critical value for percolation, but in hyperbolic geometry a different behavior occurs. The following theorem is due to Tykesson and can be found as Theorem 4.2 in [Tyk07].

Theorem 3.2.3. *For the Poisson Boolean model in $\mathbb{H}^2$ we have*

$$0 < \lambda_c < \lambda_u < \infty.$$

Moreover, with probability one the following holds.

1. *For any $\lambda \leq \lambda_c$, we have $N_{\mathcal{O}} = 0, N_{\mathcal{V}} = 1$*
2. *For any $\lambda \in (\lambda_c, \lambda_u)$, we have $N_{\mathcal{O}} = N_{\mathcal{V}} = \infty$*
3. *For any $\lambda \geq \lambda_u$, we have $N_{\mathcal{O}} = 1, N_{\mathcal{V}} = 0$.*

This type phenomenon has received a great deal of attention in the context of Bernoulli percolation on so-called non-amenable graphs. It is one of the longstanding conjectures in percolation theory to establish that there is a non-uniqueness phase for Bernoulli percolation on transitive non-amenable graphs.

The second critical value we consider here is the presence of infinite geodesics emanating from a fixed point. For a random set $\mathcal{S}$ in $\mathbb{H}^2$, let $\mathrm{Vis}(\mathcal{S})$ denote the event that there is an infinite geodesic ray emanating from o contained in $\mathcal{S}$. The critical values are then defined by

$$\lambda_{\text{ vis}} := \sup\{\lambda > 0 : \mathbb{P}_\lambda[\mathrm{Vis}(\mathcal{O}_{\mathbb{H}})] = 0\}, \tag{3.20}$$

$$\lambda^\star_{\text{vis}} := \inf\{\lambda > 0 : \mathbb{P}_\lambda[\mathrm{Vis}(\mathcal{V}_{\mathbb{H}})] = 0\} \tag{3.21}$$

In the Euclidean setting it is known that $\lambda_{\text{vis}} = \infty, \lambda^\star_{\text{vis}} = 0$ but for the hyperbolic plane we have the following theorem which is due to Benjamini, Jonasson, Schramm and Tykesson, [BJST09].

Theorem 3.2.4. *It is the case that $0 < \lambda_{vis}, \lambda^\star_{vis} < \infty$ and at the respective critical values there are no infinite geodesics.*

Theorem 3.2.4 says that for $\lambda \in (0, \lambda_{\text{vis}})$, with positive probability there exists a random direction from o in which one can move forever without hitting $\mathcal{O}_{\mathbb{H}}$. This is somewhat surprising since in any fixed direction one will hit $\mathcal{O}_{\mathbb{H}}$ with probability one.

3.3 Fractal percolation models

Fractal percolation models are in a sense scale-invariant versions of classical percolation models. They provide interesting examples of random fractals that are (relatively speaking) easy to analyze and that exhibit several interesting phenomena. A random fractal is a random set whose law is statistically self-similar in the sense that an enlargement of a small piece has the same distribution as the original set.

In this section we shall discuss the two most simple fractal percolation models, the Mandelbrot fractal percolation model and the fractal ball model.

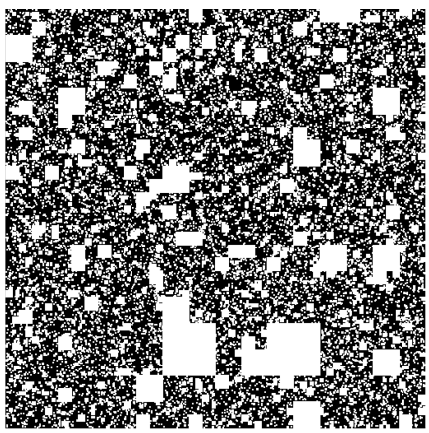

(a) The Mandelbrot percolation model.

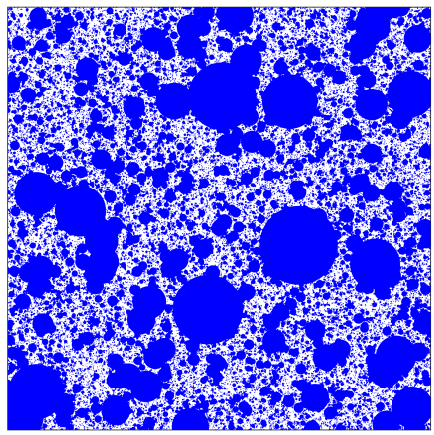

(b) The fractal ball model.

The Mandelbrot percolation model was introduced by its namesake in [Man74] as a model for turbulence. The first mathematical treatment of this model is due to Chayes, Chayes and Durrett, [CCD88]. They considered the model in the unit square, $[0, 1]^2$, but the model generalizes easily to higher dimensions. For the sake of presentation, we shall restrict ourselves to the two-dimensional case.

Informally, the model is obtained by first dividing the unit square $[0, 1]^2$ into N^2

equal squares for some integer $N \geq 2$ and then flipping a coin independently for each of the squares. If the coin shows heads we keep the square and otherwise we discard it. This produces a random set M_1. For every square in M_1, we further subdivide it into N^2 subsquares and repeat the coin flipping procedure yielding a new random set M_2. This process is then repeated indefinitely for each new square, dividing it into N^2 new squares and then flipping a coin for each such square.

The mathematical definition of the model is as follows. Let $N \geq 2$ be an integer and let $\epsilon_{i,j}^n,\ 1 \leq i,j \leq N^n, n \geq 1$ be an i.i.d sequence of Bernoulli random variables with

$$\mathbb{P}\left[\epsilon_{i,j}^n\right] = p \in (0,1),$$

and define

$$B_{i,j}^n := \left[\frac{i-1}{N^n}, \frac{i}{N^n}\right] \times \left[\frac{j-1}{N^n}, \frac{j}{N^n}\right],$$

to be the square with lower left corner $\left(\frac{i-1}{N^n}, \frac{j-1}{N^n}\right)$ and sidelength $1/N^n$.

Let

$$\mathsf{M}_1 := \bigcup_{\substack{1 \leq i,j \leq N \\ \epsilon_{i,j}^1 = 1}} B_{i,j}^1$$

and proceed inductively to define $\mathsf{M}_n, n \geq 2$ by

$$\mathsf{M}_n = \mathsf{M}_{n-1} \cap \left(\bigcup_{\substack{1 \leq i,j \leq N^n \\ \epsilon_{i,j}^n = 1}} B_{i,j}^n \right).$$

Since M_n is a decreasing sequence of compact sets Cantor's Intersection Theorem implies that the limiting set $\mathsf{M} = \cap_{n \geq 1} \mathsf{M}_n$ whenever $\mathsf{M}_n \neq \emptyset, \forall n \geq 1$.

Remark 3.3.1. *Note that if $\epsilon_{i,j}^n = 0$ then all subsquares contained within $B_{i,j}^n$ are trivially discarded. It is not hard to see that there is a one-to-one correspondence between a Galton Watson tree on an N^2 regular tree and the Mandelbrot percolation model.*

Now that the mathematical framework is up and running let us discuss what immediate questions come to mind regarding the limiting set M. The first basic question is whether

$$\mathbb{P}_{N,p}\left[\mathsf{M} = \emptyset\right] = 1, \forall p \in [0,1], N \geq 2.$$

Fortunately this is *not* the case. In [CCD88] the following elementary result was established.

Lemma 3.3.1. *For $p \leq 1/N^2$ we have*

$$\mathbb{P}_{N,p}\left[\mathsf{M} = \emptyset\right] = 1,$$

while for $p > 1/N^2$ we have

$$\mathbb{P}_{N,p}\left[\mathsf{M} \neq \emptyset\right] > 0.$$

Rephrased in terms of critical values, this theorem states that if we let p_e be the critical value

$$p_e(N) = \sup\left\{p \in [0,1] : \mathbb{P}_{N,p}\left[\mathsf{M} = \emptyset\right] = 1\right\}$$

then $p_e(N) = 1/N^2$ and $\mathbb{P}_{N,1/N^2}\left[\mathsf{M} = \emptyset\right] = 0$.

Though peripheral to their purpose in [CCD88], they also established the almost sure Hausdorff dimension of M.

Theorem 3.3.1. *If $p > 1/N^2$, then the Hausdorff dimension of M with parameters p and N is $2 + \frac{\log(p)}{\log(N)}$.*

It is a classical fact, see Proposition 3.5 on p.51 in [Fal14], that if the Hausdorff dimension of a set is strictly less than one, then the set is totally disconnected. A little algebra shows that if $p < 1/N$ then M is totally disconnected. The converse of this statement is not true, in fact M is known to be totally disconnected for $p < 1/\sqrt{N}$, see item (2) in subsection 1b of [CCD88].

Hence, the next question that is natural to ask is, what are the topological properties of M? Does it look like the Cantor set (see Figure 2.1)? That is, is it totally disconnected for all possible values of p, or are there connected components consisting of more than 1 point?

Phrasing this in terms of a critical value, we define

$$p_c(N) := \sup\left\{p \in [0,1] : \mathbb{P}_{N,p}\left[\mathsf{M} \text{ is totally disconnected }\right] = 0\right\}. \tag{3.22}$$

Worth mentioning is that in the original paper [CCD88] they initially considered a different critical value, namely

$$p_c'(N) = \sup\left\{p \in [0,1] : \mathbb{P}_{N,p}\left[\mathsf{M} \text{ has a left-right crossing in } [0,1]^2\right] = 0\right\}.$$

Theorem 2 in the same paper shows on the other hand that they coincide in

the two-dimensional case. The non-triviality of $p_c(N)$ was also established in the same article.

Theorem 3.3.2.

$$0 < p_c(N) < 1, \forall N \geq 2.$$

We can now move on to defining the fractal ball model. This model can be viewed as a semi-scale invariant version of the Poisson Boolean model.

Similarly to the Boolean model this is a Poisson point process on the following space of configurations

$$\Omega = \left\{ \omega = \sum_{i \geq 1} \delta_{(x_i, r_i)} : \omega\left(K \times [a,b]\right) < \infty, \right. \\ \left. K \times [a,b] \subset \mathbb{R}^d \times (0,1] \text{ compact } \right\}. \tag{3.23}$$

c.f. with Equation (3.8). The intensity measure of the fractal ball model is given by

$$\lambda \cdot \mathrm{Leb}_d \times \mathrm{I}\{0 < r \leq 1\} r^{-(d+1)} \mathrm{d}r, \lambda > 0. \tag{3.24}$$

The object of interest is the vacant set

$$\mathcal{V}_f := \mathbb{R}^d \setminus \bigcup_{(x,r) \in \mathrm{supp}\,(\omega)} B_d(x,r). \tag{3.25}$$

Note that a key difference when compared to the Boolean model is that the number of balls containing a point $x \in \mathbb{R}^d$ is almost surely infinite. In fact, for any $\lambda > 0$ we have

$$\mathbb{P}_\lambda\left[x \in \mathcal{V}_f\right] = 0, \forall x \in \mathbb{R}^d,$$

which by Fubinis theorem implies that the Lebesgue measure of $\mathcal{V}_f$ is almost surely 0. Analogously to the Mandelbrot percolation model this model exhibits two distinct phase transitions. The existence phase transition, defined by

$$\lambda_e = \inf\left\{\lambda > 0 : \mathbb{P}_\lambda\left[\mathcal{V}_f = \emptyset\right] = 1\right\}, \tag{3.26}$$

and the connectivity phase transition

$$\lambda_c = \inf\left\{\lambda > 0 : \mathbb{P}_\lambda\left[\mathcal{V}_f \text{ is totally disconnected }\right] > 0\right\}. \tag{3.27}$$

The result for the existence phase transition is as follows.

Theorem 3.3.3. *For any $d \geq 1$ we have $\lambda_e = d/\mathrm{Vol}\,(B_d(o,1))$ and*

$$\mathbb{P}_{\lambda_e}\left(\mathcal{V}_f = \emptyset\right) = 1.$$

The proof of this result is similar to the proof of Theorem 1.1 in Paper III, and the result is due to Broman, Jonasson and Tykesson in [BJT17], see also the paper by Bierme and Estrade [BE12].

Using Theorem 3.6 in [BE12] we can compute the Hausdorff dimension.

Theorem 3.3.4. *For $\lambda < \lambda_e$, the Hausdorff dimension of $\mathcal{V}_f$ is $d-\mathrm{Vol}\,(B_d(o,1))\lambda$ almost surely.*

The result that establishes the non-triviality of the connectivity phase is due to Broman and Camia in [BC10]. The proof is based on a coupling between the fractal ball model and the Mandelbrot percolation process.

Theorem 3.3.5. *For any $d \geq 2$ we have $\lambda_c \in (0, \infty)$ and*

$$\mathbb{P}_{\lambda_c}\left(\mathcal{V}_f \text{ is totally disconnected }\right) = 1.$$

Compared to the classical percolation models we see that the fractal models exhibits a *discontinuous* phase transition concerning the connectivity threshold λ_c. In particular, Corollary 2.6 in [BC10] shows that for any annulus $B_d(s) \setminus B_d(t), 0 < t < s < \infty$ the probability that $\mathcal{V}_f$ contains a connected component that intersects both $\partial B_d(t)$ and $\partial B_d(s)$ is discontinuous in λ at λ_c.

4 Continuum percolation models with infinite range dependencies

In this chapter we introduce the models studied in the appended papers. The models are the Brownian interlacements, the Brownian excursions, the fractal Poisson cylinder model and the random ellipsoid model. We aim to give an understanding of the models from a local point of view and for the complete technical details we refer to the appended papers.

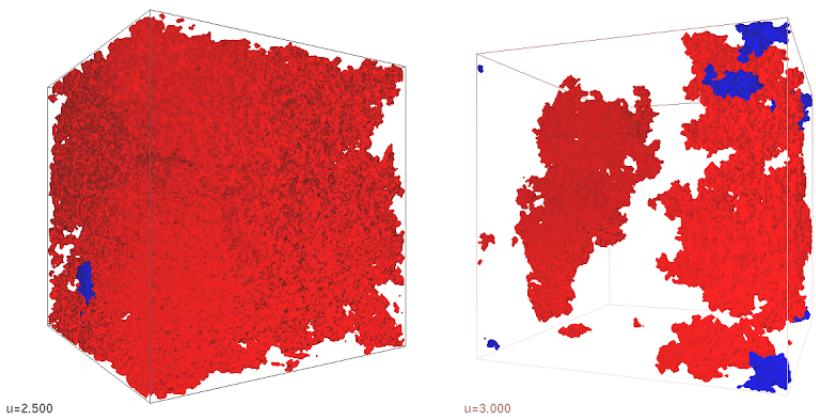

Figure 4.1: The vacant set left by a random walk on the discrete torus $(\mathbb{Z}/N\mathbb{Z})^3$ after $\lfloor uN^3 \rfloor$ steps. The largest cluster is colored red and the second largest is colored blue. Simulations due to David Windisch, see [Win].

4.1 Brownian interlacements

The Brownian interlacements is a continuum analogue of the random interlacements model. It was introduced as a means to study scaling limits of the so-called occupation time measure of the random interlacements model in [Szn13]. The random interlacements was introduced by Sznitman in [Szn10] and is a percolation model exhibiting slowly decaying infinite range dependencies.

Informally, the random interlacements model consists of a Poisson process on the space of doubly-infinite transient nearest-neighbour paths on $\mathbb{Z}^d, d \geq 3$ modulo time-shifts, which looks like two-sided simple random walks. In this way one obtains two random sets on $\mathbb{Z}^d$, the set of vertices that are covered by the trace of the Poisson process, the occupied set, and the set of vertices that are untouched, the vacant set. The development of the model was motivated by the study of disconnection times of random walks on the discrete torus $\mathbb{Z}^d \setminus N\mathbb{Z}^d$ in [BS08]. In fact, the geometry of the sites in the torus $\mathbb{Z}^d \setminus N\mathbb{Z}^d$ that are untouched by the random walk is believed to correspond to that of the vacant set of the random interlacements as N gets large, see [Win08, Szn09].

As of now this process has received a great deal of attention with numerous connections to other models in statistical mechanics such as the Gaussian free field, see for instance [Lup16, Szn12, RS13], and the wired uniform spanning forest, [Hut18]. The Brownian interlacements process on the other hand is not as well studied apart from the basic properties concerning percolation and connectivity, [Li19]

Similarly to the random interlacements the Brownian interlacements process is defined as a Poisson process on the space of doubly-infinite transient Brownian paths on $\mathbb{R}^d, d \geq 3$. To be more precise, we let W^* denote the space of bi-infinite continuous transient curves in $\mathbb{R}^d$ modulo time shifts. On W^* there exists a certain σ-finite measure ν, see Theorem 2.2 in [Szn13], which is invariant under the rotations and translations of $\mathbb{R}^d$. The Brownian interlacements process with intensity α is then defined as a Poisson point process on W^* with intensity measure $\alpha \cdot \nu, \alpha > 0$. The construction of the measure ν is quite intricate and we refer to [Szn13] for the details. Vaguely speaking the measure ν makes the trajectories look like double-sided Brownian motion paths. The parameter α governs the mean number of Brownian paths that intersects a fixed set K and plays the same role as the intensity λ in the Poisson Boolean model.

The occupied set of the Brownian interlacements (denoted by $\mathsf{BI}(\alpha, \rho)$) is then defined as the closed ρ-neighborhood of the union of the trajectories in the Brownian interlacements process. The law of the occupied set of the Brownian

interlacements, $\mathsf{BI}(\alpha, \rho)$ is then determined by

$$\mathbb{P}\left[\mathsf{BI}(\alpha, \rho) \cap K \neq \emptyset\right] = \mathrm{e}^{-\alpha \mathrm{cap}(K^\rho)}, \tag{4.1}$$

where $\mathrm{cap}(K)$ is the Newtonian capacity defined by (2.11).

A different and perhaps more intuitive description of the occupied set is the following. For simplicity we shall assume that $\rho = 0$ and write $\mathsf{BI}(\alpha) = \mathsf{BI}(\alpha, 0)$. Let $r > 0$ and let

$$N_r = N_r(\alpha) \sim \mathrm{Po}\left(\alpha \frac{2\pi^{d/2}}{\Gamma(d/2-1)} r^{d-2}\right)$$

be a Poisson random variable. Conditionally on $N_r(\alpha)$ let $X_1, ..., X_{N_r}$ be independent uniformly distributed random variables on the sphere $\partial B_d(r)$ and let $W_1, ..., W_{N_r}$ be independent Brownian motions with $W_i(0) = X_i$. Then the Brownian interlacements satisfies the following distributional equality

$$\mathsf{BI}(\alpha) \cap B_d(r) = \bigcup_{i=1}^{N_r(\alpha)} [W_i] \cap B_d(r), \tag{4.2}$$

where $[W_i] = \cup_{t \geq 0} W_i(t)$ denotes the trajectory of the Brownian motion.

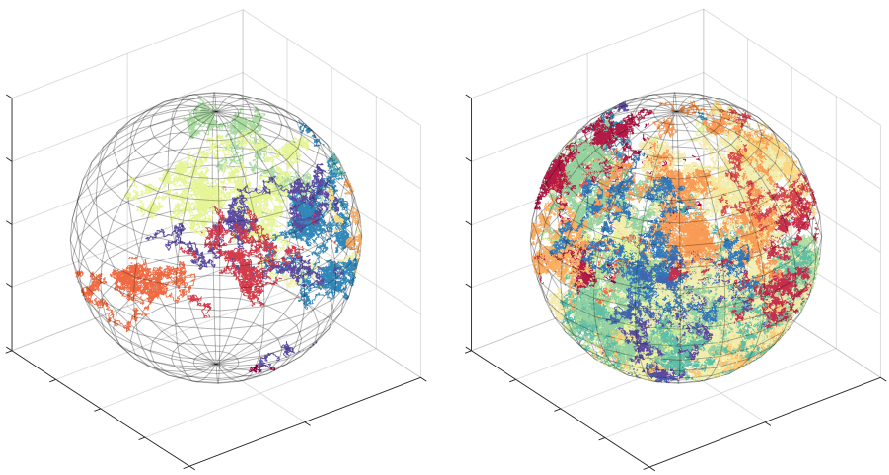

Figure 4.2: Two simulations of the Brownian interlacements in the sphere $B_3(100)$ with intensities $\alpha = 0.001$ and $\alpha = 0.015$ respectively. Different colors correspond to the different trajectories $[W_i]$ entering the local picture.

4.2 Brownian excursions

The Brownian excursion process originated as a tool for studying the intersection exponents of Brownian motion, see [LW00, LW99, LSW01]. It is a conformally invariant process and is intimately linked with the SLE(κ, ρ) curves via the theory of conformal restriction measures, see [LSW03]. It has also been shown that the Brownian excursion measure is the scaling limit of the so called simple random walk excursion measure, see [Koz06].

Concretely speaking, the Brownian excursions process in the unit disc $\mathbb{D}$ is a Poisson point process on the space of trajectories who spend their life time in $\mathbb{D}$ with endpoints on the boundary $\partial\mathbb{D}$. The intensity measure, typically referred to as the Brownian excursion measure, is a σ-finite measure and is described below.

Let $W_{\mathbb{C}}$ be the set of curves $w : [0, T_w] \to \mathbb{C}$ where $T_w \in (0, \infty)$. Then let $W_{\mathbb{D}}$ be the set of all $w \in W_{\mathbb{C}}$ such that $w(0), w(T_w) \in \partial\mathbb{D},\ w(t) \in \mathbb{D}, \forall t \in (0, T_w)$.

We equip $W_{\mathbb{C}}$ with the metric $d_{\mathbb{C}}$ defined by

$$d_{\mathbb{C}}(w, w') := |T_w - T_{w'}| + \sup_{s\in[0,1]} |w(T_w s) - w'(T_{w'} s)|\,,\ w, w' \in W_{\mathbb{C}}.$$

It is known that $W_{\mathbb{C}}$ equipped with $d_{\mathbb{C}}$ is a complete metric space, see Section 5.1 of [Law05].

For $r \in (0, 1)$, let σ_r be the uniform probability measure on $\partial B_2(r)$. Let $\mathbb{P}_{\sigma_r}$ denote the law of a Brownian motion started uniformly on the circle $\partial B_2(r)$ that is killed upon hitting the boundary $\partial\mathbb{D}$. The Brownian excursion measure on $\mathbb{D}$ is defined as the weak limit (with respect to e.g the induced Prokhorov metric)

$$\mu = \lim_{\epsilon\to 0} \frac{2\pi}{\epsilon} \mathbb{P}_{\sigma_{1-\epsilon}}. \tag{4.3}$$

We remark that μ is supported on $W_{\mathbb{D}}$. The Brownian excursions process is a Poisson process with intensity measure $\alpha \cdot \mu, \alpha > 0$. The Brownian excursions set at level α is given by the union of the trajectories in the aforementioned Poisson process and is denoted by $\mathsf{BE}(\alpha)$. Our main motivation for studying the Brownian excursion process is the fact that this can be seen as a hyperbolic analogue of the Brownian interlacements process. Indeed, in Paper II, we prove that the local picture of the Brownian interlacements and the Brownian excursions cloud are of similar flavor.

We now describe the local picture of the Brownian excursions set inside a ball.

Let $r \in (0,1)$ and let

$$N_r = N_r(\alpha) \sim \mathrm{Po}\left(\alpha \frac{2\pi}{\log(1/r)}\right)$$

be a Poisson random variable. Conditionally on N_r let

$$X_1, ..., X_{N_r}$$

be independent uniformly distributed random variables on the circle $\partial B_2(r)$ and let $W_1, ..., W_{N_r}$ be independent Brownian motions with $W_i(0) = X_i$ and that is killed upon hitting the boundary of the unit disc. Then the Brownian excursions process satisfies the following distributional equality

$$\mathsf{BE}(\alpha) \cap B_2(r) = \bigcup_{i=1}^{N_K(\alpha)} [W_i] \cap B_2(r), \tag{4.4}$$

where $[W_i]$ denotes the trajectory of the Brownian motion.

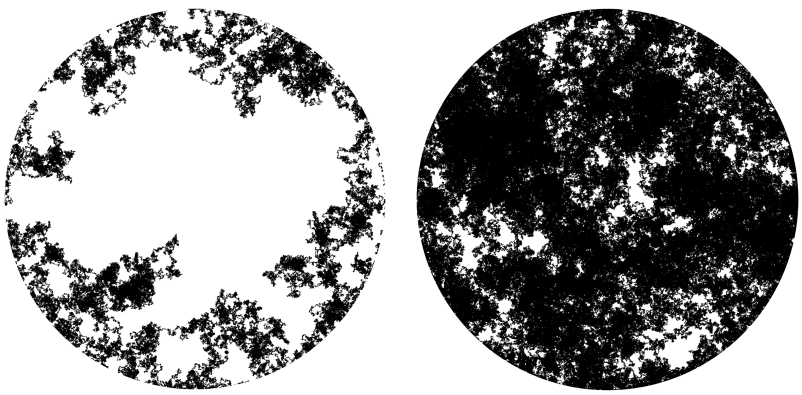

Figure 4.3: Two simulations of the Brownian excursion process with intensities $\alpha = 0.4$ and $\alpha = 1.8$ respectively. The white part is the vacant set and the black part is the occupied set.

4.3 The fractal Poisson cylinder process

The fractal cylinder process is the main actor of Paper III. Before we get into the details we recall some facts and results regarding the standard (non-fractal) Poisson cylinder process.

The regular Poisson cylinder process is a continuum percolation process which can be thought of as the natural geometrical extension of the Poisson Boolean model in the sense that we replace "points by lines". Concretely, this means that the underlying randomness now comes from a Poisson process ω on the space of affine lines on $\mathbb{R}^d$ denoted by $A(d,1)$. The intensity measure of the Poisson process is given by $\lambda \cdot \nu_d, \lambda > 0$ where ν_d is the Haar measure, that is ν_d is the canonical volume measure on on $A(d,1)$. See Example 2.4.2 for the case $d = 2$. Each line L in ω is then taken to be the central axis of a bi-infinite cylinder of radius 1. The vacant set is then given by is the complement of the union of the cylinders.

The Poisson cylinder process has been studied in the context of percolation in [TW12, HST15, BT16]. In particular, in [TW12, HST15] it is proven that the vacant set undergoes a non-trivial phase transition concerning percolation whenever $d \geq 3$. A rather contrasting behavior is proved in [BT16] concerning the occupied set. There it is proven that for any two cylinders in the Poisson cylinder model there is a sequence of at most $d-2$ other cylinders creating a connection and that there are cylinders within the model that are not connected by a sequence of at most $d-3$ other cylinders. On the applied side the Poisson line process has been used in the modeling of various properties of vehicular networks, see [CD18].

The Poisson cylinder model on $\mathbb{R}^d$ can locally be generated as follows. Let $B = [-L, L]^{d-1} \times \{0\}$ be a $d-1$-dimensional box with side length $2L > 0$ embedded in $\mathbb{R}^d$ and let $N_L \sim \mathrm{Po}\left(\lambda(2L)^{d-1}\right)$ be a Poisson random variable. Conditionally on N_L let $p^i, 1 \leq i \leq N_L$ be i.i.d random variables uniformly distributed on B. Let $a_i, 1 \leq i \leq N_L$ be i.i.d random variables on $\mathbb{R}^{d-1}$ with the probability density function, $f : \mathbb{R}^{d-1} \mapsto \mathbb{R}_+$ given by

$$f(x) = \frac{c_d}{(1 + \|x\|^2)^{\frac{d+1}{2}}}, \tag{4.5}$$

where c_d is chosen so that $\int_{\mathbb{R}^{d-1}} f(x)\mathrm{d}x = 1$. Then if we let

$$L_i := \{(a_i, 1)t + (p_i, 0) : t \in \mathbb{R}\}$$

we have that the Poisson cylinder model restricted to cylinders with center line intersecting the box B coincides in law with the union of cylinders

$$\bigcup_{i=1}^{N_L} (L_i + B_d(0,1)). \tag{4.6}$$

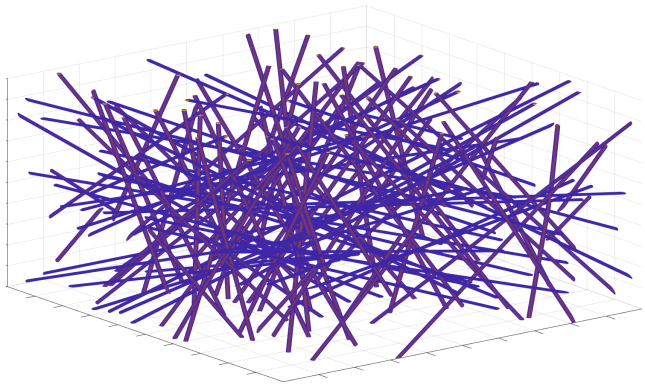

Figure 4.4: The occupied set of the Poisson cylinder model in $\mathbb{R}^3$ with intensity $\lambda = 0.003$.

The fractal cylinder model is a Poisson process on the augmented space $A(d,1) \times (0,1]$ where the second coordinate describes the cylinder radius similar to the fractal ball model, see Section 3.3. To be precise, we consider a Poisson process

$$\omega = \sum_{i \geq 1} \delta_{(L_i, r_i)}$$

on the space $A(d,1) \times (0,1]$ equipped with the intensity measure

$$\lambda \nu_d \otimes \mathrm{I}\{0 < r \leq 1\} r^{-d} \mathrm{d}r. \tag{4.7}$$

The vacant set of the fractal cylinder process is then defined by

$$\mathcal{V}(\omega) = \mathbb{R}^d \setminus \bigcup_{(L,r) \in \mathrm{supp}\,(\omega)} (L + B_d(o,r)).$$

Similar to the fractal ball model, see Section 3.3, the probability that a fixed point is in $\mathcal{V}$ is zero for any $\lambda > 0$. In particular, this implies that the Lebesgue measure of $\mathcal{V}$ is almost surely zero.

4.4 The random ellipsoid model

The random ellipsoid model is obtained by considering a Poisson cylinder model in $\mathbb{R}^d, d \geq 3$ and then intersecting it with a k-dimensional subspace. In this way one obtains a continuum percolation model depending on the two parameters

$d \geq 3$ and $k \in \{2, 3, ..., d-1\}$ as well as the intensity λ of the underlying Poisson point process on $A(d, 1)$. The random ellipsoid model resembles the Poisson Boolean model, the key difference being that one replaces the balls with ellipsoids. It appeared implicitly in one of the proofs in [TW12]. The case $k = 2$ and $d = 3$ was already studied in [TU17]. Continuum percolation models with ellipsoids has been considered within the physics community, see for instance [GSDT95, YS04, XT88].

To be precise, the random ellipsoid model is a locally finite Poisson process on the space $\mathbb{R}^k \times \mathcal{E}_{k,d}$, where $\mathcal{E}_{k,d}$ is the space of all k-dimensional ellipsoids centered at the origin. The intensity measure of the Poisson process is given by $\lambda \cdot \mathrm{Leb}_k \times \zeta_{k,d}, \lambda > 0$, where $\zeta_{k,d}$ is a shape measure on ellipsoids derived from the Poisson cylinder process. Following the same procedure as above, we write this as

$$\omega = \sum_{i \geq 1} \delta_{(z_i, E_i)}$$

and define the occupied set by

$$\mathcal{O}_E(\omega) = \bigcup_{(z,E) \in \mathrm{supp}\,(\omega)} z + E.$$

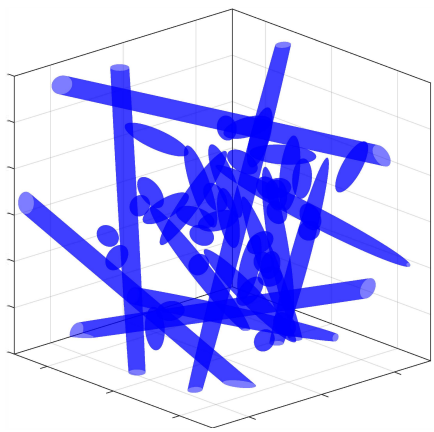

Figure 4.5: The occupied set (blue) of the random ellipsoid model with $k = 3$ and $d = 4$ simulated with centers in the box $[-10, 10]^3$ and intensity $\lambda = 0.05$.

The connected component containing the origin is defined by

$$\mathcal{C}_o(\omega) = \left\{ x \in \mathbb{R}^k : o \overset{\mathcal{O}}{\leftrightarrow} x \right\},$$

and we let $\#\mathcal{C}_o$ denote the cardinality of the set $\{(z, E) \in \omega : z + E \subset \mathcal{C}_o\}$.

One easy way of generating the random ellipsoid model is to first sample a Poisson point process on $\mathbb{R}^d$ and then to each point generate a sequence of i.i.d ellipsoids $(E_i)_{i\geq 1}$ which follows the distribution specified by Equation (17) in Paper IV. Even though the distribution has a rather cumbersome expression, the random ellipsoids are relatively easy to describe, see Lemma 6.1 and 7.7 in Paper III as well as Section 2.3 in Paper IV.

5 Summary of results

This chapter provides a summary of the results of the four papers included in the thesis. Papers I and II as well as III and IV are related both chronologically as well as thematically.

5.1 Paper I

In the first paper [ET19] we studied the topic of visibility in the vacant set of the Brownian interlacements and the Brownian excursions process. The problem of visibility in a random set $\mathcal{S}$ (with isometry-invariant law) can be thought of as placing a person at a fixed point o and asking how far this person can see in *some* direction within this set, without having the view obstructed by the complement of $\mathcal{S}$. Heuristically, if this random set is in some sense very irregular or erratic we should expect a rapid decay of the probability that the person has visibility to a distance r.

Formally, we say that the visibility from o in $\mathcal{S}$ is at least r if there is some line-segment of length r starting at o contained in $\mathcal{S}$. The probability of this event is denoted by $P_{vis}(r)$. The probability that a fixed line-segment of length r is contained in $\mathcal{S}$ is denoted by $f(r)$. In other words, $f(r)$ is the probability of having visibility to distance at least r in a *fixed* direction Our two main results concerning the Brownian interlacements and excursions processes are two rather contrasting behaviours, reflecting the difference between Euclidean and hyperbolic geometry. Suppose now that $\mathcal{S}$ is the vacant set of the Brownian interlacements model. We obtain estimates on $P_{vis}(r)$ in terms of $f(r)$.

Theorem 5.1.1 (Theorem 2.2 in [ET19])**.** *There exist constants* $0 < c < c' < \infty$

depending only on d, ρ and α such that

$$P_{vis}(r) \leq cr^{2(d-1)} f(r), d \geq 3 \tag{5.1}$$
$$P_{vis}(r) \geq c' r^{d-1} f(r), d \geq 4 \tag{5.2}$$

for r large enough.

For the Brownian excursion process we obtain a different behavior, showing that it undergoes a phase transition in terms of visibility to infinity, determining the critical value and what happens at the critical value. Let V_∞^α denote the event that there exists an infinite geodesic (with respect to the the hyperbolic metric) from a fixed point, o, contained in the vacant set of the Brownian excursion process.

Theorem 5.1.2 (Theorem 2.3 in [ET19])**.** *It is the case that*

$$\mathbb{P}\left(V_\infty^\alpha\right) > 0, \ \alpha < \pi/4, \tag{5.3}$$
$$\mathbb{P}\left(V_\infty^\alpha\right) = 0, \ \alpha \geq \pi/4. \tag{5.4}$$

5.2 Paper II

Paper II is devoted to computing the critical value concerning percolation in the vacant set, $\mathcal{V} = \mathbb{D} \setminus \mathsf{BE}(\alpha)$, of the Brownian excursions process in the unit disc. Using results on conformal restriction measures and SLE curves we can determine the critical value and what happens at the critical value.

Let

$$\alpha_c = \inf\left\{\alpha > 0 : \mathbb{P}_\alpha\left[o \overset{\mathcal{V}}{\leftrightarrow} \partial\mathbb{D}\right] = 0\right\},$$

be the critical value for the event that the origin is in an unbounded (with respect to the hyperbolic metric) connected component of $\mathcal{V}$.

Theorem 5.2.1 (Theorem 1.1 in [EVT19])**.** *The vacant set of the Brownian excursion process has a non-trivial phase transition concerning percolation and the critical value of the phase transition is given by*

$$\alpha_c = \pi/3.$$

Moreover, at α_c the component of $\mathcal{V}$ containing the origin is almost surely finite.

Combining these results with the results from Paper I we see the following

- For any $\alpha < \pi/4$, with positive probability there exist infinite geodesics in $\mathcal{V}$ emanating from o.
- For any $\pi/4 \leq \alpha < \pi/3$, with positive probability $\mathcal{V}$ percolates but there are no infinite geodesics emanating from o.
- For any $\alpha \geq \pi/3$, all components of $\mathcal{V}$ are finite almost surely.

Here, "infinite" is with respect to the hyperbolic metric on $\mathbb{D}$.

5.3 Paper III

Paper III deals with phase transitions in the fractal Poisson cylinder model defined in Section 4.3. Let $\mathcal{V}$ denote the vacant set left by the fractal cylinder model and define the following critical values

$$\lambda_e := \inf\{\lambda > 0 : \mathbb{P}(\mathcal{V} = \emptyset) = 1\}, \tag{5.5}$$

$$\lambda_c := \inf\{\lambda > 0 : \mathbb{P}(\mathcal{V} \text{ is totally disconnected }) > 0\}. \tag{5.6}$$

Our main results concerning these thresholds are the following two theorems:

Theorem 5.3.1 (Part of Theorem 1.1 and Theorem 1.7 in [BEMT19]). *For any $d \geq 2$ we have $\lambda_e = d$ and the fractal is in the empty phase at criticality. Moreover for $\lambda < d$ the Hausdorff dimension of $\mathcal{V}$ is $d - \lambda$ almost surely.*

Theorem 5.3.2 (Theorem 1.3 in [BEMT19]). *For $d \geq 4$, we have that $\lambda_c \in (0, \infty)$. For $d = 3$, then $\mathcal{V} \cap \mathbb{R}^2$ almost surely does not contain any connected components for any $\lambda > 0$. For $d = 2$ we have that $\lambda_c = 0$.*

One interesting phenomenon in these fractal models in comparison with the regular percolation models is that we have three intervals, $\lambda < \lambda_c$, $\lambda \in (\lambda_c, \lambda_e)$, $\lambda \geq \lambda_e$ with three distinct behaviors:

$\lambda < \lambda_c$	$\lambda_c < \lambda < \lambda_e$	$\lambda \geq \lambda_e$
There exist connected components in $\mathcal{V}$ containing more than one point	All components in $\mathcal{V}$ are totally disconnected	The fractal is in the empty phase, i.e. $\mathcal{V} = \emptyset$.

In the proofs of these results we derive a new continuum percolation model which we refer to as the *random ellipsoid model.* This model is essential in proving the non-triviality of the connectivity phase transition.

Theorem 5.3.3 (Part of Theorem 1.5 in [BEMT19]). *Consider the Poisson cylinder model in $\mathbb{R}^d$ with cylinder radius r. The intersection of this cylinder process to the subspace $\mathbb{R}^k$ where $k \in \{1, \dots, d-1\}$ is a Poisson process of ellipsoids with intensity measure*

$$\lambda \cdot \mathrm{Leb}_k \times \xi_{k,r}, \lambda > 0. \tag{5.7}$$

Here $\xi_{k,r}$ is a finite measure on the space of ellipsoids centered at the origin. In fact $\xi_{k,r}$ is the non-normalized version of $\zeta_{k,d}$ in Section 4.4.

5.4 Paper IV

Paper IV analyzes the random ellipsoid model which was derived in Paper III. The main theorem shows a dichotomous behavior for the following thresholds:

$$\lambda_{\mathrm{perc}}(k) = \inf\left\{\lambda > 0 : \mathbb{P}_\lambda\left[o \overset{\mathcal{O}_E}{\leftrightarrow} \infty\right] > 0\right\}, \tag{5.8}$$

$$\lambda_{\mathrm{cross}}(k) = \inf\left\{\lambda > 0 : \inf_{r>0} \mathbb{P}_\lambda\left[B_k(r) \overset{\mathcal{O}_E}{\leftrightarrow} B_k(2r)^c\right] > 0\right\}, \tag{5.9}$$

$$\lambda_N(k) = \sup\left\{\lambda > 0 : \mathbb{E}_\lambda\left[\#\mathcal{C}_o\right] < \infty\right\}. \tag{5.10}$$

Theorem 5.4.1 (Theorem 1.1 of [Eli19]). *For $k \in \{2, 3, ..., \lfloor d/2 \rfloor\}$ we have*

$$0 < \lambda_{\mathrm{cross}}, \lambda_N \leq \lambda_{\mathrm{perc}} < \infty \tag{5.11}$$

while for $k \in \{\lfloor d/2 \rfloor + 1, ..., d-2\}$ we have

$$0 = \lambda_{\mathrm{cross}} < \lambda_N \leq \lambda_{\mathrm{perc}} < \infty. \tag{5.12}$$

Moreover, $\lambda_N(d-1) = 0$.

Bibliography

[ATT18a] Daniel Ahlberg, Vincent Tassion, and Augusto Teixeira. Existence of an unbounded vacant set for subcritical continuum percolation. *Electron. Commun. Probab.*, 23:Paper No. 63, 8, 2018.

[ATT18b] Daniel Ahlberg, Vincent Tassion, and Augusto Teixeira. Sharpness of the phase transition for continuum percolation in $\mathbb{R}^2$. *Probab. Theory Related Fields*, 172(1-2):525–581, 2018.

[Bal87] Isaac Balberg. Recent developments in continuum percolation. *Philosophical Magazine B*, 56(6):991–1003, 1987.

[BC10] Erik I. Broman and Federico Camia. Universal behavior of connectivity properties in fractal percolation models. *Electron. J. Probab.*, 15:1394–1414, 2010.

[BE12] Hermine Biermé and Anne Estrade. Covering the whole space with Poisson random balls. *ALEA Lat. Am. J. Probab. Math. Stat.*, 9:213–229, 2012.

[Bef08] Vincent Beffara. The dimension of the SLE curves. *Ann. Probab.*, 36(4):1421–1452, 2008.

[BEMT19] Erik Broman, Olof Elias, Filipe Mussini, and Johan Tykesson. The fractal cylinder process: existence and connectivity phase transition. *Preprint*, August 2019.

[BH57] S. R. Broadbent and J. M. Hammersley. Percolation processes. I. Crystals and mazes. *Proc. Cambridge Philos. Soc.*, 53:629–641, 1957.

[BJST09] Itai Benjamini, Johan Jonasson, Oded Schramm, and Johan Tykesson. Visibility to infinity in the hyperbolic plane, despite obstacles. *ALEA Lat. Am. J. Probab. Math. Stat.*, 6:323–342, 2009.

[BJT17] Erik I. Broman, Johan Jonasson, and Johan Tykesson. The existence phase transition for two Poisson random fractal models. *Electron. Commun. Probab.*, 22:Paper No. 21, 8, 2017.

[BK89] R. M. Burton and M. Keane. Density and uniqueness in percolation. *Comm. Math. Phys.*, 121(3):501–505, 1989.

[BP17] Christopher J. Bishop and Yuval Peres. *Fractals in probability and analysis*, volume 162 of *Cambridge Studies in Advanced Mathematics*. Cambridge University Press, Cambridge, 2017.

[BR06] Béla Bollobás and Oliver Riordan. *Percolation*. Cambridge University Press, New York, 2006.

[BS08] Itai Benjamini and Alain-Sol Sznitman. Giant component and vacant set for random walk on a discrete torus. *J. Eur. Math. Soc. (JEMS)*, 10(1):133–172, 2008.

[BT16] Erik I. Broman and Johan Tykesson. Connectedness of Poisson cylinders in Euclidean space. *Ann. Inst. Henri Poincaré Probab. Stat.*, 52(1):102–126, 2016.

[CCD88] J. T. Chayes, L. Chayes, and R. Durrett. Connectivity properties of Mandelbrot's percolation process. *Probab. Theory Related Fields*, 77(3):307–324, 1988.

[CD18] V. V. Chetlur and H. S. Dhillon. Coverage analysis of a vehicular network modeled as cox process driven by poisson line process. *IEEE Transactions on Wireless Communications*, 17(7):4401–4416, July 2018.

[CFKP97] James W. Cannon, William J. Floyd, Richard Kenyon, and Walter R. Parry. Hyperbolic geometry. In *Flavors of geometry*, volume 31 of *Math. Sci. Res. Inst. Publ.*, pages 59–115. Cambridge Univ. Press, Cambridge, 1997.

[CLR79] J Chalupa, P L Leath, and G R Reich. Bootstrap percolation on a bethe lattice. *Journal of Physics C: Solid State Physics*, 12(1):L31–L35, jan 1979.

[CR85] M. Campanino and L. Russo. An upper bound on the critical percolation probability for the three-dimensional cubic lattice. *Ann. Probab.*, 13(2):478–491, 1985.

[DCT16] Hugo Duminil-Copin and Vincent Tassion. A new proof of the sharpness of the phase transition for Bernoulli percolation on $\mathbb{Z}^d$. *Enseign. Math.*, 62(1-2):199–206, 2016.

[DRT18] Hugo Duminil-Copin, Aran Raoufi, and Vincent Tassion. Subcritical phase of d-dimensional Poisson-Boolean percolation and its vacant set. *arXiv e-prints*, page arXiv:1805.00695, May 2018.

[Eli19] Olof Elias. Properties of a random ellipsoid model. *Preprint*, December 2019.

[ET19] Olof Elias and Johan Tykesson. Visibility in the vacant set of the Brownian interlacements and the Brownian excursion process. *ALEA Lat. Am. J. Probab. Math. Stat.*, 16(2):1007–1028, 2019.

[EVT19] Olof Elias, Fredrik J. Viklund, and Johan Tykesson. Percolation of the vacant set of the brownian excursions process. *Preprint*, December 2019.

[Fal14] Kenneth Falconer. *Fractal geometry*. John Wiley & Sons, Ltd., Chichester, third edition, 2014. Mathematical foundations and applications.

[FLM19] James Foster, Terry Lyons, and Vlad Margarint. An asymptotic radius of convergence for the Loewner equation and simulation of SLE_k traces via splitting. *arXiv e-prints*, page arXiv:1912.06424, Dec 2019.

[Fos19] James Foster. sle-simulation. `https://https://github.com/james-m-foster/sle-simulation`, 2019.

[Gil61] E. N. Gilbert. Random plane networks. *J. Soc. Indust. Appl. Math.*, 9:533–543, 1961.

[Gil65] E. N. Gilbert. The probability of covering a sphere with N circular caps. *Biometrika*, 52:323–330, 1965.

[Gou08] Jean-Baptiste Gouéré. Subcritical regimes in the Poisson Boolean model of continuum percolation. *Ann. Probab.*, 36(4):1209–1220, 2008.

[Gri99] Geoffrey Grimmett. *Percolation*, volume 321 of *Grundlehren der Mathematischen Wissenschaften [Fundamental Principles of Mathematical Sciences]*. Springer-Verlag, Berlin, second edition, 1999.

[GSDT95] E. J. Garboczi, K. A. Snyder, J. F. Douglas, and M. F. Thorpe. Geometrical percolation threshold of overlapping ellipsoids. *Phys. Rev. E*, 52:819–828, Jul 1995.

[Hal85] Peter Hall. On continuum percolation. *Ann. Probab.*, 13(4):1250–1266, 1985.

[HS90] Takashi Hara and Gordon Slade. Mean-field critical behaviour for percolation in high dimensions. *Comm. Math. Phys.*, 128(2):333–391, 1990.

[HST15] M. R. Hilário, V. Sidoravicius, and A. Teixeira. Cylinders' percolation in three dimensions. *Probab. Theory Related Fields*, 163(3-4):613–642, 2015.

[Hut18] Tom Hutchcroft. Interlacements and the wired uniform spanning forest. *Ann. Probab.*, 46(2):1170–1200, 2018.

[HvdH17] Markus Heydenreich and Remco van der Hofstad. *Progress in high-dimensional percolation and random graphs.* CRM Short Courses. Springer, Cham; Centre de Recherches Mathématiques, Montreal, QC, 2017.

[HW65] J. M. Hammersley and D. J. A. Welsh. First-passage percolation, subadditive processes, stochastic networks, and generalized renewal theory. In *Proc. Internat. Res. Semin., Statist. Lab., Univ. California, Berkeley, Calif*, pages 61–110. Springer-Verlag, New York, 1965.

[Kak44] Shizuo Kakutani. Two-dimensional Brownian motion and harmonic functions. *Proc. Imp. Acad. Tokyo*, 20:706–714, 1944.

[Kes80] Harry Kesten. The critical probability of bond percolation on the square lattice equals $\frac{1}{2}$. *Comm. Math. Phys.*, 74(1):41–59, 1980.

[Koz06] Michael J. Kozdron. On the scaling limit of simple random walk excursion measure in the plane. *ALEA Lat. Am. J. Probab. Math. Stat.*, 2:125–155, 2006.

[Law05] Gregory F. Lawler. *Conformally invariant processes in the plane*, volume 114 of *Mathematical Surveys and Monographs.* American Mathematical Society, Providence, RI, 2005.

[Li19] Xinyi Li. Percolative Properties of Brownian Interlacements and Its Vacant Set. *Journal of Theoretical Probability*, September 2019.

[LSW01] Gregory F. Lawler, Oded Schramm, and Wendelin Werner. Values of Brownian intersection exponents. I. Half-plane exponents. *Acta Math.*, 187(2):237–273, 2001.

[LSW03] Gregory Lawler, Oded Schramm, and Wendelin Werner. Conformal restriction: the chordal case. *J. Amer. Math. Soc.*, 16(4):917–955, 2003.

[Lup16] Titus Lupu. From loop clusters and random interlacements to the free field. *Ann. Probab.*, 44(3):2117–2146, 2016.

[LW99] Gregory F. Lawler and Wendelin Werner. Intersection exponents for planar Brownian motion. *Ann. Probab.*, 27(4):1601–1642, 1999.

[LW00] Gregory F. Lawler and Wendelin Werner. Universality for conformally invariant intersection exponents. *J. Eur. Math. Soc. (JEMS)*, 2(4):291–328, 2000.

[Man74] Benoit B. Mandelbrot. Intermittent turbulence in self-similar cascades: divergence of high moments and dimension of the carrier. *Journal of Fluid Mechanics*, 62(2):331–358, 1974.

[Man75] Benoit B Mandelbrot. *Les objets fractals: forme, hasard et dimension.* Flammarion, 1975.

[Man82] Benoît B. Mandelbrot. *The fractal geometry of nature.* Freeman, 1982.

[Men86] M. V. Menshikov. Coincidence of critical points in percolation problems. *Dokl. Akad. Nauk SSSR*, 288(6):1308–1311, 1986.

[MP10] Peter Mörters and Yuval Peres. *Brownian motion*, volume 30 of *Cambridge Series in Statistical and Probabilistic Mathematics*. Cambridge University Press, Cambridge, 2010. With an appendix by Oded Schramm and Wendelin Werner.

[MR96] Ronald Meester and Rahul Roy. *Continuum percolation*, volume 119 of *Cambridge Tracts in Mathematics*. Cambridge University Press, Cambridge, 1996.

[RS05] Steffen Rohde and Oded Schramm. Basic properties of SLE. *Ann. of Math. (2)*, 161(2):883–924, 2005.

[RS13] Pierre-François Rodriguez and Alain-Sol Sznitman. Phase transition and level-set percolation for the Gaussian free field. *Comm. Math. Phys.*, 320(2):571–601, 2013.

[Sah94] Muhammad Sahimi. *Applications of percolation theory.* Taylor & Francis, 1994.

[Sar97] Anish Sarkar. Co-existence of the occupied and vacant phase in Boolean models in three or more dimensions. *Adv. in Appl. Probab.*, 29(4):878–889, 1997.

[Sch00] Oded Schramm. Scaling limits of loop-erased random walks and uniform spanning trees. *Israel J. Math.*, 118:221–288, 2000.

[SW08] Rolf Schneider and Wolfgang Weil. *Stochastic and integral geometry*. Probability and its Applications (New York). Springer-Verlag, Berlin, 2008.

[Szn98] Alain-Sol Sznitman. *Brownian motion, obstacles and random media*. Springer Monographs in Mathematics. Springer-Verlag, Berlin, 1998.

[Szn09] Alain-Sol Sznitman. Random walks on discrete cylinders and random interlacements. *Probab. Theory Related Fields*, 145(1-2):143–174, 2009.

[Szn10] Alain-Sol Sznitman. Vacant set of random interlacements and percolation. *Ann. of Math. (2)*, 171(3):2039–2087, 2010.

[Szn12] Alain-Sol Sznitman. Random interlacements and the Gaussian free field. *Ann. Probab.*, 40(6):2400–2438, 2012.

[Szn13] Alain-Sol Sznitman. On scaling limits and Brownian interlacements. *Bull. Braz. Math. Soc. (N.S.)*, 44(4):555–592, 2013.

[TU17] Augusto Teixeira and Daniel Ungaretti. Ellipses percolation. *J. Stat. Phys.*, 168(2):369–393, 2017.

[TW12] Johan Tykesson and David Windisch. Percolation in the vacant set of Poisson cylinders. *Probab. Theory Related Fields*, 154(1-2):165–191, 2012.

[Tyk07] Johan Tykesson. The number of unbounded components in the Poisson Boolean model of continuum percolation in hyperbolic space. *Electron. J. Probab.*, 12:no. 51, 1379–1401, 2007.

[Wer05] Wendelin Werner. Conformal restriction and related questions. *Probab. Surv.*, 2:145–190, 2005.

[Wer09] Wendelin Werner. Lectures on two-dimensional critical percolation. In *Statistical mechanics*, volume 16 of *IAS/Park City Math. Ser.*, pages 297–360. Amer. Math. Soc., Providence, RI, 2009.

[Wie23] Norbert Wiener. Differential-space. *Journal of Mathematics and Physics*, 2(1-4):131–174, 1923.

[Win] David Windisch. The vacant set left by a random walk on a discrete torus. [Online]. Available from: `https://sites.google.com/site/dwindisch/torus1`. [Accessed 27rd October 2019].

[Win08] David Windisch. Random walk on a discrete torus and random interlacements. *Electron. Commun. Probab.*, 13:140–150, 2008.

[Wu15] Hao Wu. Conformal restriction and Brownian motion. *Probab. Surv.*, 12:55–103, 2015.

[XT88] W. Xia and M. F. Thorpe. Percolation properties of random ellipses. *Phys. Rev. A*, 38:2650–2656, Sep 1988.

[YS04] Y. B. Yi and A. M. Sastry. Analytical approximation of the percolation threshold for overlapping ellipsoids of revolution. *Proceedings: Mathematical, Physical and Engineering Sciences*, 460(2048):2353–2380, 2004.

[Zie18] Sebastian Ziesche. Sharpness of the phase transition and lower bounds for the critical intensity in continuum percolation on $\mathbb{R}^d$. *Ann. Inst. Henri Poincaré Probab. Stat.*, 54(2):866–878, 2018.